JOURNAL OF QUATERNARY SCIENCE (2021) **36**(7) 1174–1189 ISSN 0267-8179. DOI: 10.1002/jqs.3359

JQS Journal of Quaternary Science QRA Quaternary Research Association

Chronology of the Mediterranean sea-level highstand during the Last Interglacial: a critical review of the U/Th-dated deposits

FRANCESCA PASQUETTI,[1]* MONICA BINI,[1,2,3] BIAGIO GIACCIO,[4] ANDREA RATTI,[1] MATTEO VACCHI[1] and GIOVANNI ZANCHETTA[1,2,4]

[1]Department of Earth Sciences, University of Pisa, Pisa, Italy
[2]CIRSEC, Centre for Climatic Change Impact, University of Pisa, Pisa, Italy
[3]INGV, Istituto Nazionale di Geofisica e Vulcanologia, Pisa, Italy
[4]IGAG-CNR, Institute of Environmental Geology and Geoengineering, Monterotondo, Rome, Italy

Received 15 March 2021; Revised 23 June 2021; Accepted 20 July 2021

ABSTRACT: Relative sea-level (RSL) evolution during Marine Isotopic Stage (MIS) 5 in the Mediterranean basin is still not fully understood despite a plethora of morphological, stratigraphic and geochronological studies carried out on highstand deposits of this area. In this review we assembled a database of 323 U/Th-dated samples (e.g. corals, molluscs, speleothems) which were used to chronologically constrain RSL evolution within MIS 5. The application of strict geochemical criteria to the U/Th samples indicates that only ~33% of data available for the Mediterranean Sea can be considered 'reliable'. Most of these data (~65%) refer to the MIS 5e highstand, while only ~17% could be related to the MIS 5a. No attribution to MIS 5c can be unequivocally supported. Nevertheless, the resulting framework does not allow us to define a satisfactory RSL trend during the MIS 5e highstand and subsequent MIS 5 substages. Overall, the proposed selection of reliable/unreliable data would be useful for detecting areas where MIS 5 substage attributions are not supported by confident U/Th chronological data and thus the related reconstructions need to be revised. In this regard, the resulting framework calls for a reappraisal and re-examination of the Mediterranean records with advanced geochronological methodologies.

KEYWORDS: Last Interglacial highstand; Mediterranean Sea; sea-level changes; Tyrrhenian; U/Th dating

Introduction

The increasing concentration of greenhouse gases in the atmosphere is leading the Earth's climate towards warmer conditions with consequent sea-level rise resulting from ice melting and ocean expansion (Clark *et al.*, 2016; Steffen *et al.*, 2018). This makes the study of past interglacial periods particularly important to have a pre-anthropogenic scenario of a warmer climate (Tzedakis *et al.*, 2009; Burke *et al.*, 2018). However, the definition of the conditions distinguishing an interglacial period is not trivial and evades a tight definition. For the last ~800 ka, according to a pragmatic notion recently provided by the Past Interglacials Working Group of PAGES (2016), an interglacial is a period characterized by the absence of substantial Northern Hemisphere ice outside Greenland. If we exclude the current interglacial, the Last Interglacial (LIG) period is the best-known interglacial for the amount of data available (e.g. Dutton and Lambeck, 2012; Govin *et al.*, 2015; Tzedakis *et al.*, 2018). On the basis of sea-level variations, constrained by U/Th dating of corals on different far field sites (i.e. regions located far from the polar ice-sheets) (e.g. Dutton and Lambeck, 2012), the LIG covers approximately the time-interval between 129 and 116 ka (e.g. Stirling *et al.*, 1998; Muhs, 2002) with global mean sea-level which peaked up to 5–10 m above that of the present day (e.g. Kopp *et al.*, 2009; Dutton and Lambeck, 2012; Dutton *et al.*, 2015). However, the timing, duration and millennial-scale oscillations of sea-level within the LIG remain controversial (Stirling *et al.*, 1998; Hearty *et al.*, 2007; O'Leary *et al.*, 2013; Rohling *et al.*, 2019) and represent a major focus of ongoing sea-level research (Rovere *et al.*, 2020). An accurate chronological constraint of the global spatiotemporal variability of sea-level represents the fundamental basis to improve our current knowledge on its evolution in this key interglacial period.

Mediterranean coasts preserve many sedimentary and geomorphological features commonly correlated to the LIG highstand which are found at different elevations according to variable tectonics and glacio- and hydro-isostatic adjustment (GIA, Ferranti *et al.*, 2006; Stocchi *et al.*, 2018). This LIG highstand has been locally termed 'Tyrrhenian' (see the review by Asioli *et al.*, 2005 and references therein; Issel 1914). Specifically, Issel (1914) defined the Tyrrhenian with reference to geological sections of beach deposits outcropping in southern Sardinia, and containing warm-water molluscs. The importance of these sedimentary occurrences in the Mediterranean coastal area, and in particular in southern Italy, has also suggested that they can be used to define a Global Boundary Stratigraphic Section and Point (GSSP) for the formal Middle-to-Upper Pleistocene boundary. In particular, a circumstantiated proposal was performed in the Taranto area (Negri *et al.* 2015) based on the extensive presence of *Persististrombus latus* (formerly *Strombus bubonius*, e.g. Taviani 2014), a gastropod of the '*Senegalensis* warm fauna' typically identified within the Tyrrhenian deposits (Issel 1914; Hillaire-Marcel *et al.* 1996; Asioli *et al.* 2005; see also Antonioli *et al.*, 2018). The Tyrrhenian has been historically separated into at least two phases of relative sea-level (RSL) highstands (Bonifay and Mars,), the 'Eutyrrhenian' and the 'Neotyrrhenian'. Recent

*Correspondence: F. Pasquetti, as above.
Email: francesca.pasquetti@dst.unipi.it

advances in radioisotope dating methods and the definition of the Marine Isotope Stage (MIS) scale for correlating on-land successions with deep-sea marine isotopic curves (Shackleton, 1969) yielded an age of ~125 ka for the 'Eutyrrhenian', which strictly matches MIS 5e. The 'Neotyrrhenian' is thought to be either ~100 or ~80 ka, matching either MIS 5a or MIS 5c (e.g. Hillaire-Marcel *et al.*, 1996). The question is somewhat controversial because in some cases MIS 5 attributions have been made in the absence of direct dating of the littoral/marine deposits or on the basis of dates whose quality and reliability have not been verified (e.g. Federici and Mazzanti, 1995; Ambert, 1999; Conchon, 1999; Dubar *et al.*, 2008). The use of misleading data has practical consequences for local- and regional-scale reconstructions, some of which are of fundamental importance, for instance for estimation of uplift rates and consideration of local tectonic evolution (Mauz, 1999; Nisi *et al.*, 2003; Sarti *et al.*, 2005). A good example is presented by the island of Mallorca where Muhs *et al.* (2015), through an accurate selection of coral dating, showed that the Eutyrrhenian and Neotyrrhenian deposits have the same age range (~128–116 ka) and represent only different lithofacies. U/Th dating of phreatic overgrowths on speleothems (POS) on Mallorca indicate that the LIG RSL highstand was at 2.15 ± 0.75 m a.s.l during the period between 126.6 ± 0.4 and 116 ± 0.8 ka (Polyak *et al.*, 2018). Moreover, Dorale *et al.* (2010) showed a phase of POS deposition at ~1 m above present level at ~81 ka, during MIS 5a, indicating that two relative highstands may exist in this island.

Therefore, despite the many studies on LIG coastal deposits in the Mediterranean basin and improvement of the definition of the indicative meaning of sea-level markers (e.g. Antonioli *et al.*, 2015; Rovere *et al.*, 2016; Lorscheid *et al.*, 2017; Stocchi *et al.*, 2018), considerable uncertainty still exists on the chronological attribution of many successions (e.g. Bini *et al.*, 2020) and consequently on the fluctuations of RSL within the LIG as well as on the timing and duration of the highstand (e.g. Dabrio *et al.*, 2011; Muhs *et al.*, 2015; Sivan *et al.*, 2016; Marra *et al.*, 2019).

In this paper, we present and discuss a compilation of U/Th samples used to date LIG deposits along the Mediterranean coasts. Although different approaches have been employed to date the LIG shorelines [e.g. amino acid racemization (AAR) (Hearty *et al.*, 1986a,1986b); optical stimulated luminescence (OSL) (Mauz, 1999); uranium series dating on corals and molluscs (Hillaire-Marcel *et al.*, 1986, 1996)], we focused our review on U/Th dating, which is the most common method applied not only locally but also globally for the LIG (Muhs, 2002; Stirling *et al.*, 1998 among others). In this compilation we include different types of U/Th-dated samples (e.g. corals, molluscs, speleothems) to summarize as completely as possible the available data on MIS 5 sea-level evolution in the Mediterranean. However, owing to well-known factors that can affect the reliability of U/Th ages, especially for molluscs (e.g. U-mobility during the early diagenesis of marine carbonates and detrital ^{232}Th contamination), the main aim of this paper is to assess the quality and reliability of these data by applying a geochemical screening (e.g. Medina-Elizalde, 2013; Muhs *et al.*, 2015; Hibbert *et al.*, 2016) on the entire dataset. We are aware that the reliability of U/Th dates on marine molluscs remains of debate (e.g. Govin *et al.*, 2015), but we decided to include them as a further proof, to avoid the possible reiteration of chronological attribution based on this controversial material. Thus, the purpose of this paper is to provide a reliable chronological context which will help to better deal with the large amount of MIS 5 sea-level data within the Mediterranean basin. Moreover, the proposed selection of data could be useful to detect areas where MIS 5 attributions are not still supported by confident chronological data (at least for U/Th) and where future chronological investigations (eventually supported by different methodological approaches) should be addressed.

Methods

Study area and original source of data

The study area encompasses the entire Mediterranean basin (Fig. 1), an area for which there are many studies on palaeo sea-level changes, thanks to the relatively small tidal-range and low wave-energy that have allowed the preservation of a wide range of RSL markers (Lambeck and Bard, 2000; Vacchi *et al.*, 2016). In this study, we only reviewed palaeo-shorelines dated with U/Th techniques and with an age spanning from

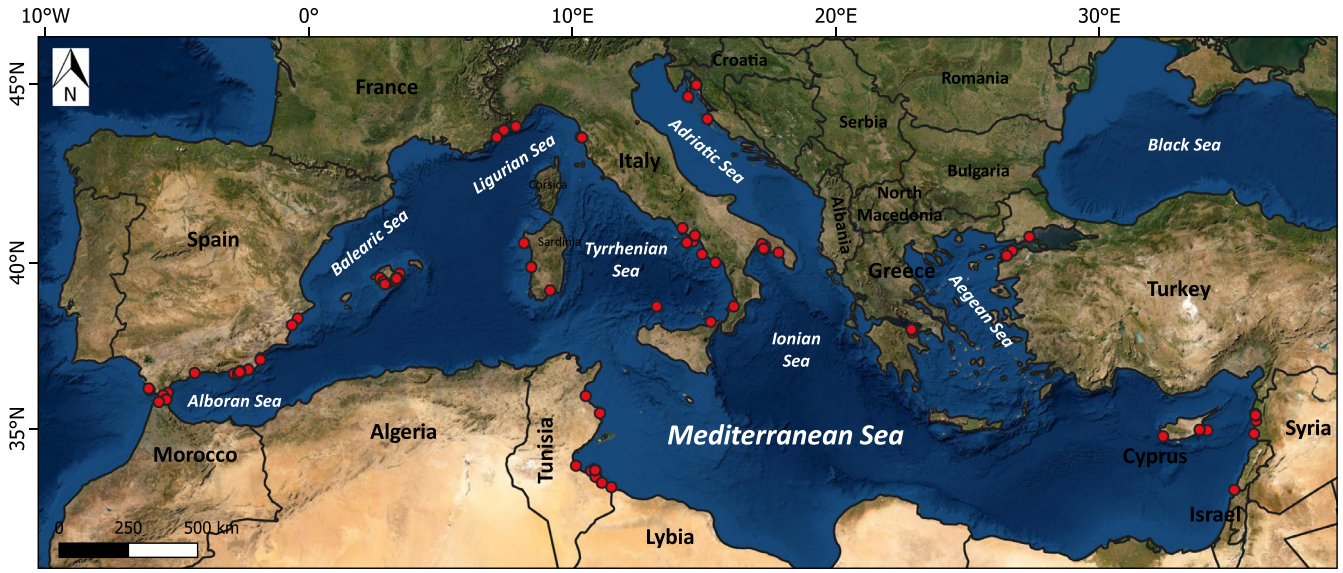

Figure 1. Extent of the study area. Red dots show the position of palaeo-RSL indicators collected in this study. The cartographic base is a world imagery provided by the ArcGIS Map Server (https://www.arcgis.com/). The country boundaries are provided by the Esri Geospatial Cloud, ArcGIS Hub (https://hub.arcgis.com/)). [Color figure can be viewed at wileyonlinelibrary.com]

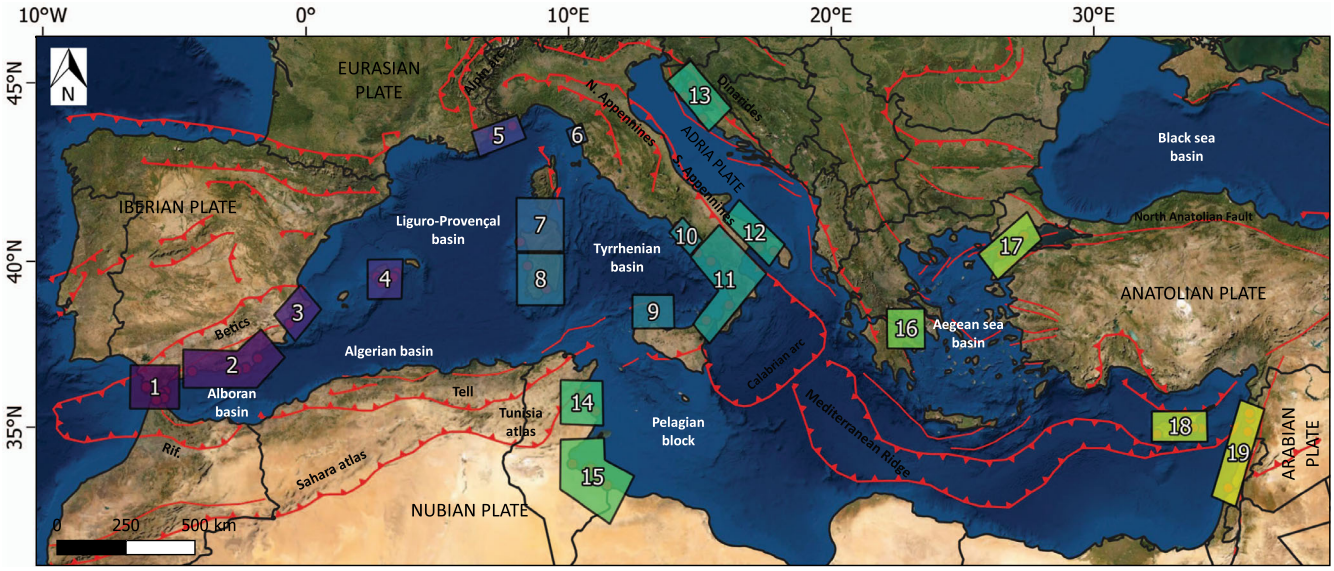

Figure 2. Simplified tectonic framework of the Mediterranean basin (faults are modified after Faccenna *et al.*, 2014). Polygons indicate the location of palaeo-RSL indicators for this study grouped on the basis of geographical position and tectonic framework. The cartographic base is a world imagery provided by the ArcGIS Map Server (https://www.arcgis.com/). [Color figure can be viewed at wileyonlinelibrary.com]

60 to 160 ka (Fig. 1). This interval, in a very broad sense, spans from late MIS 6 to the end of MIS 5 and early MIS 4 (e.g. Lisiecki and Raymo, 2005; Railsback *et al.*, 2015).

The Mediterranean is a complex geological area with large portions characterized by significant tectonic activity related to different geodynamic regimes (Fig. 2) (e.g. Nocquet, 2012; Faccenna *et al.*, 2014). The eastern sector is characterized by more intense tectonics as indicated by the strong historical seismicity and crustal deformation recorded in this area (Roberts *et al.*, 2009; Serpelloni *et al.*, 2013; Galli, 2020). The western sector is generally characterized by less intense tectonic activity, although the Tyrrhenian side of the Calabrian Arc and the central-southern Apennines have been affected by strong historical seismicity (e.g. Billi *et al.*, 2011; Faccenna *et al.*, 2014).

We clustered the data into 19 regions on the basis of their geographical position and regional tectonic setting. These areas are listed in Table 1 and shown in Fig. 2.

Database compilation

RSL markers and palaeo-RSL

We compiled available literature data to collect original data (e.g. Ratti, 2019). We then compared and integrated the collected data with those reported in the World Atlas of Last Interglacial Shorelines (WALIS, https://warmcoasts.eu/ – updated 15 December 2020), a sea-level database developed by the ERC Starting Grant 'WARMCOASTS' (ERC-StG-802414) in collaboration with the PALSEA (PAGES/INQUA) working group. For most western Mediterranean shorelines, the type of RSL marker and the value of palaeo-RSL were updated with data reported in WALIS. For data that were not included in that database, we strictly followed the same classification and calculation criteria. Therefore, for information about the classification of RSL markers and the calculation of palaeo-RSL, the reader is referred to the documentation related to WALIS.

The database presented here (see Supplementary files) includes both RSL index-points (e.g. data which constrain sea level in time and space) and RSL limiting points (e.g. data which constrain sea-level above or below a given datum; Shennan *et al.*, 2015; Rovere *et al.*, 2016).

Dating information and screening criteria

For each marker collected in our database we reported the type of dated material (e.g. mollusc, coral, speleothem), its relationship to the RSL index/limiting point (where it was collected, its elevation, etc.) and the calculated age (uncorrected age) with its related uncertainties (at 1σ or 2σ). All U/Th geochemical data reported in the initial publications were recorded in the database. These data include: ^{238}U[1], ^{232}Th[2] and ^{230}Th concentrations, the value of $\delta^{234}U_{measured}$[3], activity ratio of $^{230}Th/^{238}U$ (or $^{230}Th/^{234}U$) and, when available, activity ratio of $^{230}Th/^{232}Th$ and the value of $\delta^{234}U_{initial}$ (which indicates the value of $\delta^{234}U$ at the time of carbonate precipitation). Uncertainties in these data were included where possible. We also recorded the analytical techniques (alpha-spectrometry, TIMS or MC-ICPMS) used for analysis, decay constants used and method of spike calibration. Where available we reported the calcite content and the methodology used for this determination.

All values of $\delta^{234}U_{initial}$ were recalculated using the formula:

$$\delta^{234}U_{initial} = (\delta^{234}U_{measured})e^{(\lambda_{234}T)}$$

where $\delta^{234}U_{measured}$ is the measured value, λ_{234} is the decay constant of ^{234}U (Cheng *et al.*, 2013) and T is the age of the samples in years.

It is well known that several factors can affect the reliability of the calculated age to result in a misleading RSL chronology (e.g. Dutton, 2015). For example, the samples used for dating may have undergone diagenetic effects or may have been

[1]It was assumed that uranium concentration reported as [U] refers to [^{238}U]. When the concentration of ^{238}U was reported in d.p.m. g^{-1}, it was converted p.p.m., multiplying it by 1.35. This multiplication factor is based on the conversion factors of 1 d.p.m. = 60 Bq and 1 Bq kg^{-1} = 81 p.p.b. ^{238}U (IAEA, 1989).

[2]It was assumed that thorium concentration reported as [Th] refers to [^{232}Th]. When the concentration of ^{232}Th was reported in d.p.m. g^{-1}, it was converted to p.p.b., multiplying it by 4100. This multiplication factor is based on the conversion factors of 1 d.p.m. = 60 Bq and 1 Bq kg^{-1} = 246 p.p.b. ^{232}Th (IAEA, 1989).

[3]When the $^{234}U/^{238}U$ activity ratio was reported, it was converted in the standard delta notation according to the following equation: $\delta^{234}U_{measured} = [(^{234}U/^{238}U) - 1] \times 1000$ (Chutcharavan *et al.*, 2018).

Table 1. List of areas where data were clustered and original references

Area ID	Site	References
1	Gibraltar Strait (Spanish and Moroccan coast)	(Zazo *et al.*, 1999; El Kadiri *et al.*, 2010; Abad *et al.*, 2013; El Abdellaoui *et al.*, 2016)
2	Southern Spain (from Málaga to Almería)	(Hillaire-Marcel *et al.*, 1986; McLaren and Rowe, 1996; Zazo *et al.*, 1999)
3	Central Spain (Alicante area)	(Goy *et al.*, 2006; Hearty, 1986.)
4	Island of Mallorca, Spain	(Stearns and Thurber, 1965; Hearty, 1986; Hillaire-Marcel *et al.*, 1996; McLaren and Rowe, 1996; Vesica *et al.*, 2000; Zazo *et al.*, 2003; Tuccimei *et al.*, 2007; Dorale *et al.*, 2010; Muhs *et al.*, 2015; Polyak *et al.*, 2018)
5	Western coast of the Ligurian Sea	(Stearns and Thurber, 1965; Dubar *et al.*, 2008; Gilli, 2018)
6	Leghorn plain, Tuscany, Italy	(Nisi *et al.*, 2003; Zanchetta *et al.*, 2019)
7	Northern coast of Sardinia, Italy	(Tuccimei *et al.*, 2007)
8	Southern coast of Sardinia, Italy	(Hearty, 1986; D'Orefice *et al.*, 2012; Carboni *et al.*, 2014; Coltorti *et al.*, 2015)
9	Ustica Island, north-western Sicily, Italy	(De Vita *et al.*, 1998)
10	Salerno Bay, Campania, Italy	(Brancaccio *et al.*, 1978; Barra *et al.*, 1991; Romano *et al.*, 1994)
11	Cilento-Calabrian coast, Italy	(Hearty, 1986; Dai Pra *et al.*, 1993; Iannace *et al.*, 2001; Esposito *et al.*, 2003; Bini *et al.*, 2020)
12	Apulia coast, Italy	(Dai Pra and Stearns, 1977; Hearty, 1986; Belluomini *et al.*, 2002; Amorosi *et al.*, 2014)
13	Croatian coast	(Surić and Juračić, 2010)
14	Northern coast of Tunisia	(McLaren and Rowe, 1996)
15	Southern coast of Tunisia	(Jedoui *et al.*, 2003)
16	Corinth and Perachora peninsula, Greece	(Vita-Finzi, 1993; Dia *et al.*, 1997; Leeder *et al.*, 2005, 2003; Andrews *et al.*, 2007; Roberts *et al.*, 2009)
17	Strait of Çanakkale/Dardanelles, Turkey	(Yaltirak *et al.*, 2002)
18	Cyprus Island	(Poole *et al.*, 1990)
19	Syrian and Israeli coast	(Dodonov *et al.*, 2008; Sivan *et al.*, 2016)

contaminated with detrital ^{232}Th, resulting in erroneous ages (e.g. Gallup *et al.*, 1994; Stirling and Andersen, 2009). For U/Th dating, as for any radiometric dating method, one of the conditions to obtain reliable results is that the considered sample has remained a 'closed-system' with respect to U-series decay nuclides, which means that it has not exchanged isotopes with the surrounding environment after deposition (Broecker, 1963; Dutton, 2015). It is well known that molluscs do not incorporate significant amounts of uranium from seawater during growth and rarely remain a closed system during their post-emergence history, with the consequence that most of the uranium found in these organisms has accumulated during diagenetic processes (e.g. Kaufman *et al.*, 1971; McLaren and Rowe, 1996; Goy *et al.*, 2006). By contrast, living corals take up high uranium concentrations during growth and are less affected by diagenetic processes (e.g. Muhs *et al.*, 2015). Therefore, whereas molluscs can only be assigned to a specific interglacial, corals can provide more precise time series for the LIG (Govin *et al.*, 2015). Relative to corals and molluscs, the dense calcite of speleothems seems to be less susceptible to post-depositional alteration and thus give rise to more reliable and precise ages (Dumitru *et al.*, 2020), but nevertheless high uncertainties could be related to detrital Th incorporation (Govin *et al.*, 2015).

However, geochemical alteration of the samples and violation of the principles of the method (e.g. absence of Th at time of carbonate precipitation) can be identified by different approaches, such as: alteration of aragonite to calcite for aragonitic organisms; anomalous ^{232}Th concentrations; anomalous ^{238}U concentrations for marine organisms compared to modern analogous; and values of $\delta^{234}U_{initial}$ significantly different from those of modern seawater (Dutton and Lambeck, 2012; Medina-Elizalde, 2013; Hibbert *et al.*, 2016). Therefore, four geochemical screening criteria, which are described below and summarized in Table 2, were applied to the stored data.

Calcite content

Aragonite is meta-stable in surficial conditions and can convert to calcite over time. During this conversion, U/Th geochemistry may be altered. Therefore, for aragonitic fossil specimens it is good practice to determine the mineralogical composition of the samples, which allows us to detect the amount of calcite and thus the potential effect of diagenesis. In this study, we chose to reject samples with measured calcite abundances >3%, which is a common limit used in some original papers (e.g. Hillaire-Marcel *et al.*, 1986; El Abdellaoui *et al.*, 2016). Samples were rejected also when the calcite content was not determined. Mineralogical screening criteria were applied to aragonite marine organisms such as corals, algae and some species of molluscs.

Anomalous ^{238}U concentration

If there has been no addition/loss of uranium since the time of formation of the marine organisms, uranium concentration of the fossil should be similar to the concentration found in modern organisms of the same species. In modern corals, uranium concentration is species-dependent (Hibbert *et al.*, 2016). *Cladocora caespitosa* (L.) is the main colonial coral endemic

Table 2. Summary of geochemical screening criteria applied to chronological data

Criteria	Applied to	Threshold (acceptable values)
1. Calcite content	Aragonite marine elements	<3%
2. ^{238}U concentration	Corals	1.9–4.3 p.p.m.
	Molluscs	<1 p.p.m.
3. $\delta^{234}U_{initial}$ value	Marine elements	145 ± 10‰
4. Detrital Th	Carbonate samples	^{230}Th/^{232}Th activity ratio >40

to the Mediterranean basin used for dating (Montagna *et al.*, 2007). Modern specimens of this coral from the western Mediterranean shown U contents of 2.5–3.3 p.p.m. (Goy *et al.*, 2006), while some specimens from the northern Adriatic Sea shown a wider range between ~1.9 and ~4.3 p.p.m. (Montagna *et al.*, 2007). Therefore, to take into account the variability for this coral in the Mediterranean Sea and considering that LIG corals could have U concentrations quite different from modern values (e.g. Raddatz *et al.*, 2014; Chen *et al.*, 2021), we chose to reject coral samples with ^{238}U concentrations outside the range of 1.9–4.3 p.p.m. Unlike corals, molluscs do not take up significant amounts of U from seawater during growth. It is known that the uranium in these shells is also taken up *post mortem* (Kaufman *et al.*, 1971; Dutton, 2015). According to Ivanovich *et al.* (1983), modern mollusc shells generally contain <0.5 p.p.m. U, while fossil shells record an average of 1 p.p.m. regardless of age. Allyev and Sari (2003) detected uranium concentration of 0.034–0.65 p.p.m. for recent mollusc shells of different species. Therefore, mollusc samples with ^{238}U concentrations >1 p.p.m. were rejected.

Initial uranium isotope composition ($\delta^{234}U_{initial}$)

Corals are thought to precipitate their skeletons with no fractionation between ^{234}U and ^{238}U (Delanghe *et al.*, 2002). Thus, the $\delta^{234}U_{initial}$ value of corals should be close to that of seawater at the time of growth, if the corals have not been geochemically altered. Seawater δ^{234}U is thought to be homogeneous and relatively invariant across timescales, although some authors have suggested variations in the order of ~10–15‰ during glacial–interglacial timescales (Henderson, 2002; Esat and Yokoyama, 2006; Durand *et al.*, 2013) with values lower than modern seawater during glacial periods and values similar to the modern one for interglacial periods. Therefore, for interglacial periods, corals with $\delta^{234}U_{initial}$ values significantly different from those of modern seawater should be rejected because they are probably altered. The modern δ^{234}U seawater value determined by Andersen *et al.* (2010) is 146.8 ± 0.1‰, while Chutcharavan *et al.* (2018) report a value of 145 ± 1.5‰. Moreover, the latter authors suggest use of 145 ± 8‰ as screening values for corals younger than 17 ka (and thus of the modern interglacial period). Since the age of the collected data spans 60–160 ka, we chose to reject data with values outside a slightly wider range of 145 ± 10‰. Even molluscs should reflect isotopic seawater composition (Fortunato, 2016); the same range was thus applied to molluscs and to the other dated marine organisms (e.g. algae).

Detrital Th (^{232}Th)

The U/Th method relies on the fact that thorium is almost insoluble, and therefore initial ^{232}Th and ^{230}Th concentrations in the carbonate archive should be negligible and any ingrowth of ^{230}Th is the result of the uranium decay chain (Dutton, 2015). However, because thorium tends to be adsorbed on the surface of sedimentary particles, it could be added to the carbonate through detrital contamination. Evaluating the presence of ^{232}Th to assess potential ^{230}Th contamination relies on the fact that all Th isotopes have identical chemical properties. Therefore, if ^{232}Th is present, even a certain amount of ^{230}Th should be introduced in the carbonate (Dutton *et al.*, 2017). In previous studies, ^{230}Th/^{232}Th activity ratio values were used rather than ^{232}Th concentrations. Values greater than 40 have generally been used to indicate that the influence of detrital thorium was negligible (McLaren and Rowe, 1996). In some cases, ^{232}Th concentration was the only value reported in the original papers. In this situation, we calculated the ^{230}Th/^{232}Th activity ratio using the value of ^{230}Th obtained from the ratio ^{230}Th/^{238}U or ^{230}Th/^{234}U and the U content (all calculations were made with elements reported in Bq kg^{-1}). Then, samples with values lower than 40 were rejected. As a precaution, if none of these parameters were available (^{230}Th/^{232}Th activity ratio or ^{232}Th concentration), samples were rejected.

Each criterion was applied to the entire selected dataset to evaluate the data quality for each parameter. For each criterion we considered as reliable all the values for which at least 50% of the uncertainty range was within the threshold, which means that the average value must be within the range. Finally, all the data outside the threshold even for a single criterion were excluded from the entire dataset.

Because methods for correction were proposed by the original authors (see Discussion), for the sake of clarity, we also reported in the database the corrected age, the type of correction applied and whether the data were accepted by the original authors.

Results

Data statistics and palaeo-RSL

The database includes 323 samples which were used to date 168 markers including RSL index points and sea-level limiting points (multiple samples may have been used for dating a single RSL marker). As shown in Fig. 3(A), data mainly derive from Spain (41%), especially from the island of Mallorca (area

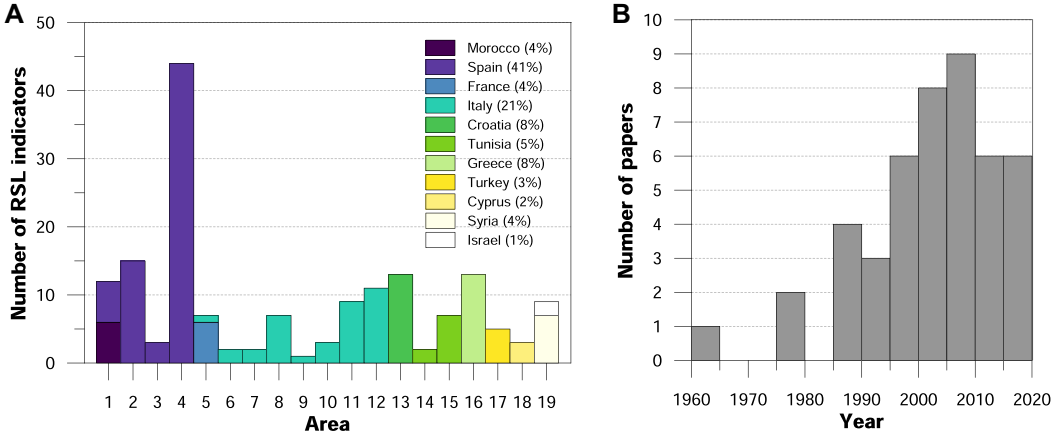

Figure 3. Geographical distribution and years of publication of the papers of the studies on Mediterranean LIG. (A) Number of RSL indicators per area (see Fig. 1 for the meaning of the numbers); (B) number of papers per year. [Color figure can be viewed at wileyonlinelibrary.com]

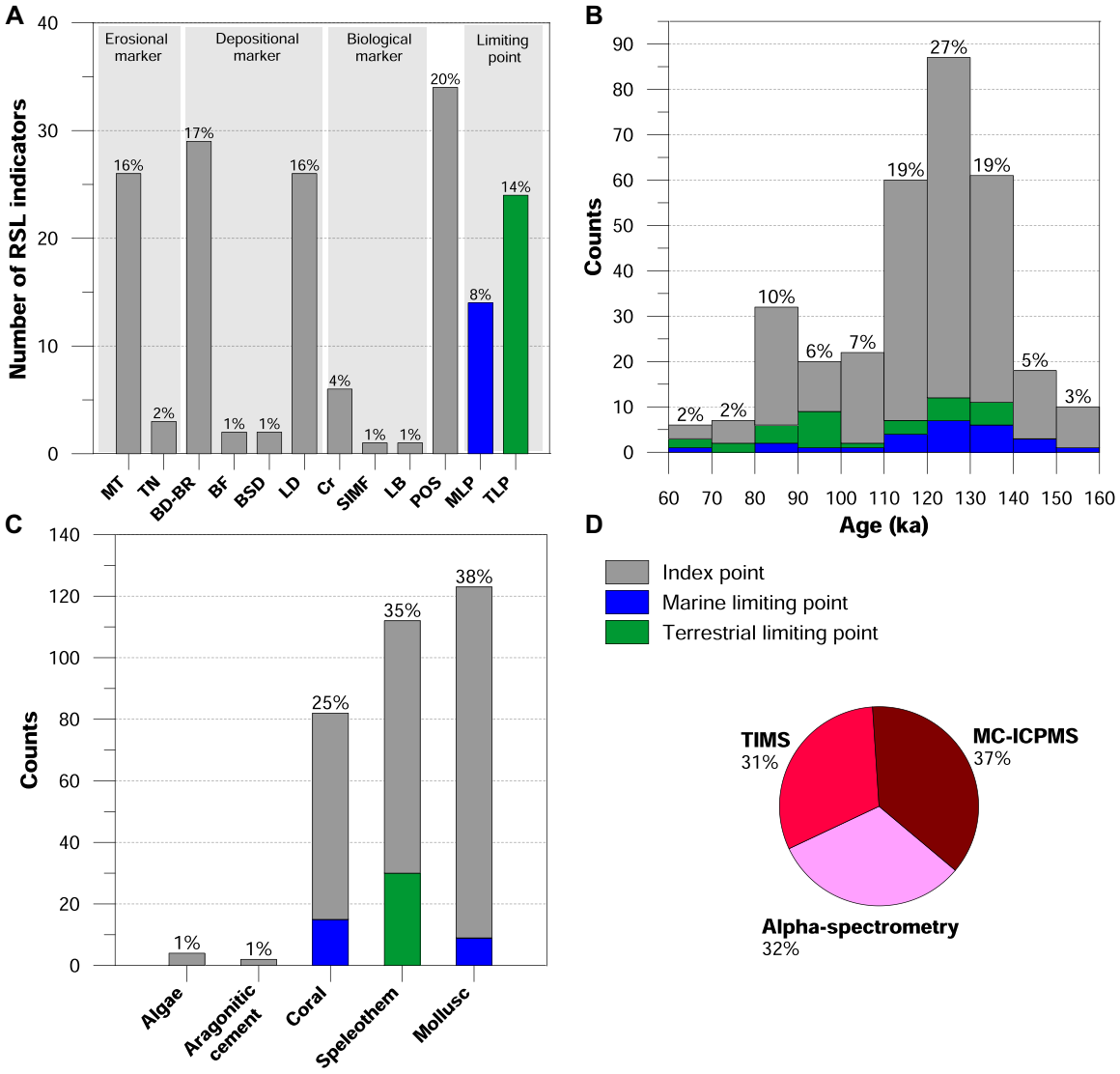

Figure 4. Statistics and data distribution. (A) Number and percentage of RSL markers grouped per classes (MT: marine terrace; TN: tidal notch; BD-BR: beach deposit or beachrock; BF: beach face; BSD: beach swash deposit; LD: littoral deposit; Cr: corals; SIMF: shallow or intertidal marine fauna; LB: upper limit of *Lithophaga* boreholes; POS: phreatic overgrowth on speleothems; MLP: marine limiting point; TLP: terrestrial limiting point). (B) Age distribution of datapoints and percentage of the different ranges. (C) Type, number and percentage of material used to date the different RSL indicators. (D) Percentage of analytical techniques adopted to date the material. In A, B and C index and limiting points are highlighted by different colours. [Color figure can be viewed at wileyonlinelibrary.com]

4; Fig. 2), and Italy (21%). According to Fig. 3(B) most of the U/Th age determinations were performed after 1985.

Most RSL indicators (35%) were derived from marine and littoral deposits (Fig. 4A). POS (e.g. Tuccimei *et al.*, 2007) and erosional indicators also constitute a large percentage of the collected data, 20 and 18%, respectively (Fig. 4A). Biological markers, which include corals (*Cladocora caespitosa*) found in growth position, the upper limit of *Lithophaga* boreholes and other kind of shallow or intertidal marine fauna, constitute only 5% of the dataset. About 22% of the data is represented by marine and terrestrial limiting points. Most terrestrial limiting points are constituted by vadose speleothems that are generally in close relationship with other RSL markers, such as speleothems covering *Lithophaga* boreholes. The age distribution of the dated samples (Fig. 4B) indicates that 65% of the data has an age ranging between 110 and 140 ka. As shown in Fig. 4(C), the dated samples are mainly represented by molluscs (38%), followed by speleothems (including vadose speleothems and POS, 35%) and corals (25%). The remaining 2% comprises calcareous algae and marine phreatic aragonite cements. Different kinds of mollusc species have been dated (*Persististrombus latus*, *Glycymeris* sp., *Ostraea* sp., *Arca* sp., etc.), while *Cladocora caespitosa* prevails among the corals. With regard to the analytical techniques used to date the material, Fig. 4(D) indicates a uniform distribution among alpha-spectrometry, TIMS and MC-ICPMS methods.

Figure 5 shows the elevation of the reconstructed RSL using the U/Th-dated markers included in our dataset. As shown, most of the index points (~83%) have values between 0 and 20 m above modern mean sea level (MSL), with 66% of the data distributed between 0 and 10 m and the remaining 17% between 10 and 20 m. For the index points the highest values (up to 59.9 m) were detected in the most tectonically active areas of the Mediterranean basin (areas 9–17) while negative values (down to −16.5 m) derived from POS found below the modern MSL in the Mallorca caves (area 4). The elevation of marine and terrestrial limiting points is instead between −50 and 30 m above modern MSL.

Geochemical screening test

Figure 6 reports the four geochemical screening criteria applied to the chronological data. As summarized in Table 2, criterion 1 (calcite content) was applied to aragonitic marine

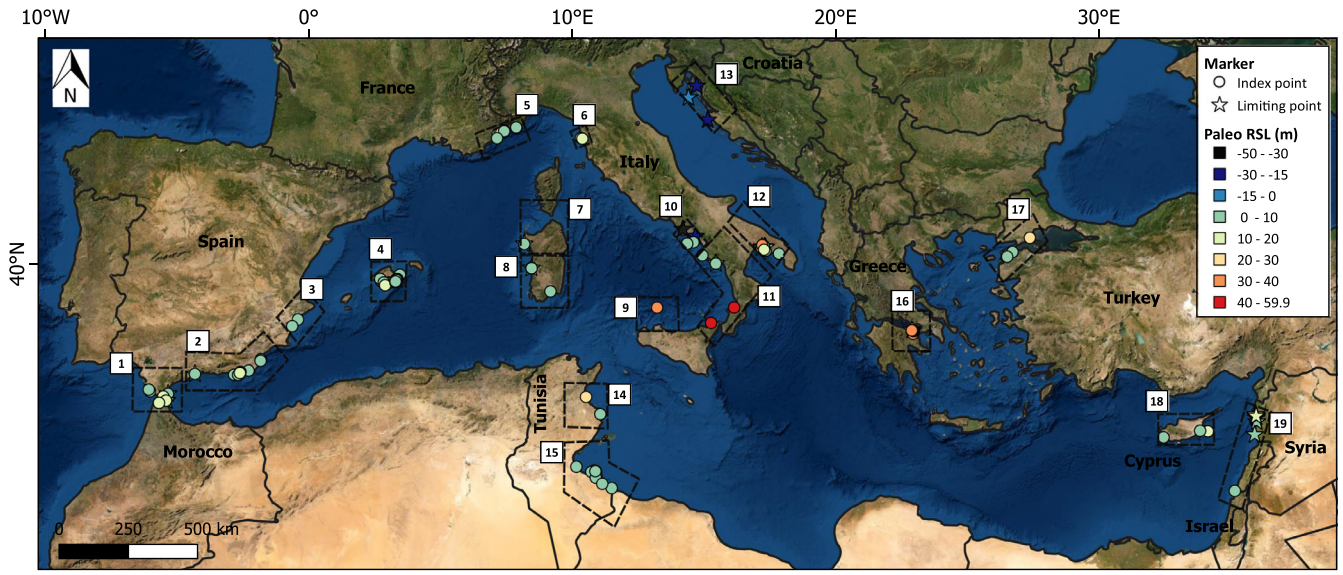

Figure 5. Palaeo-RSL (m) of the markers included in the dataset. Index points are represented by dots while limiting points are represented by stars. The different colour of the datapoints indicates the range of their elevation in agreement with the colour-scale shown in the key. [Color figure can be viewed at wileyonlinelibrary.com]

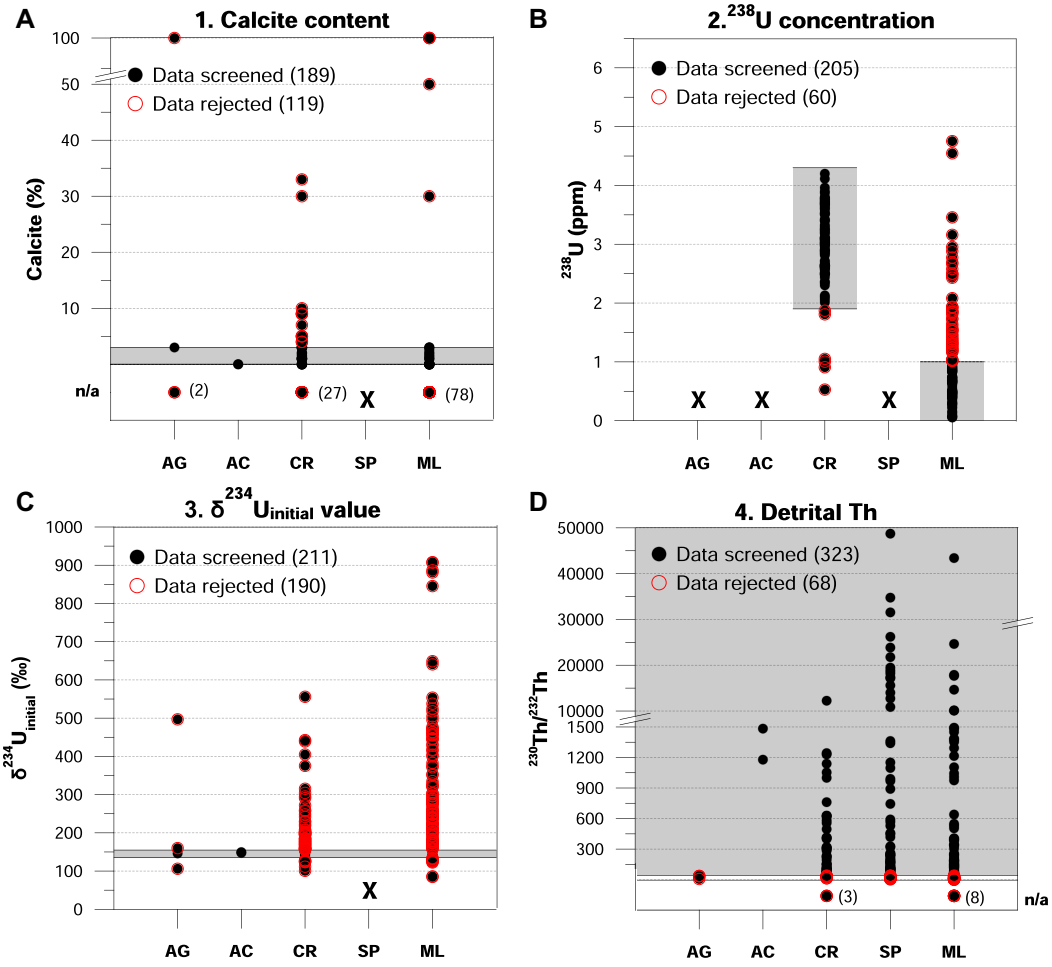

Figure 6. Geochemical screening criteria applied to the chronological data summarized in Table 1: (A) calcite content; (B) ^{238}U concentration; (C) δ^{234}U initial value; (D) detrital Th. The types of dated material (AG: algae; AC: aragonitic cement; CR: corals; SP: speleothems; ML: molluscs) are reported on the *x*-axis. The 'X' above a group of dated material indicates that it is excluded from screening analysis. Black dots represent screened data for each criterion, while red circles represent rejected data (number of datapoints in parentheses). Non-available data (n/a) are reported below the zero line of the *y*-axis (number of datapoints in parentheses). Grey stripes denote the range of acceptable values: (1) calcite contents <3%; (2) ^{238}U concentrations between 1.9 and 4.3 p.p.m. for corals and <1 p.p.m. for molluscs; (3) δ^{234}U initial values included in the range 145 ± 10‰; (4) ^{230}Th/^{232}Th activity ratio >40. [Color figure can be viewed at wileyonlinelibrary.com]

specimens (algae, aragonitic cement, corals and some species of molluscs) for 189 samples, criterion 2 (^{238}U concentration) was applied to corals and molluscs for 205 samples, criterion 3 ($\delta^{234}U_{initial}$ value) was applied to marine elements (algae, aragonitic cement, corals and molluscs) for 211 samples, and criterion 4 (detrital Th) was applied to carbonate samples and thus to the entire dataset (323 samples). For calcite content (Fig. 6A), 119 out of 189 samples (~63% of the screened data) were rejected. Among the rejected data, the majority (107 samples) were rejected because calcite content was not determined in the original papers (n/a in Fig. 6A). For ^{238}U concentration (Fig. 6B) 60 samples of corals and molluscs were rejected (~29% of the screened data). The $\delta^{234}U_{initial}$ value (Fig. 6C) was the most selective criterion. Only 10% of the 211 screened samples passed the threshold of 145 ± 10‰, while the remaining 90% were rejected (190 samples). As shown in Fig. 6(C), molluscs were the most variable with $\delta^{234}U_{initial}$ values up to ~908‰. For detrital Th (Fig. 6D) about 21% of the data were rejected (68 samples). Among these, only 11 samples were rejected because neither ^{230}Th/^{232}Th activity ratio nor ^{232}Th concentration was reported in the original papers (n/a Fig. 6D).

By combining the four different criteria, about 67% of the data were rejected from the dataset. The remaining 108 samples were referred to 55 sea-level data (Fig. 7A). As shown in Fig. 7(B), most of the remaining data consist of markers for which the dated material was a speleothem. Therefore, POS prevailed, constituting 58% of the remaining sea-level data (Fig. 7A). The samples which passed the screening test were mainly acquired by MC-ICPMS analytical techniques, followed by TIMS and then by alpha-spectrometry (Fig. 7C). Figure 8 shows the RSL data that passed the screening test. As reported, the ages span from ~65 to ~150 ka with data concentrated in the intervals 110–130 ka (~63%) and 80–90 ka (~16%). The highest elevation of palaeo-RSL (33 ± 5 m MSL) is still most likely to be related to post-depositional tectonic movements (area 16, Fig. 9), while negative values derived from the POS of Mallorca (area 4, Fig. 9). About 11% of the uncorrected ages rejected in this study were also rejected by the original authors. Another 29% of the data rejected in this study were accepted by the original authors after correcting the age with an open-system model or specific initial ^{230}Th/^{232}Th activity ratio value (e.g. Thompson *et al.*, 2003; Hellstrom, 2006). The remaining 60% of the data were instead accepted by the original authors.

The analyses performed by alpha-spectrometry were further removed from the final dataset, owing to the large uncertainties associated with the measurements acquired with this method, even if this does not necessarily mean they are incorrect. Indeed, current analytical techniques are now two to four orders of magnitude more efficient than the originally used alpha-spectrometric techniques (Li *et al.*, 1989; Stirling *et al.*, 2001; Hellstrom, 2003). Figure 10 shows the final result, consisting of 95 U/Th dates referred to 44 RSL indicators. In this case, 73% of the data were constituted by POS, 23% by terrestrial limiting points and the remaining 4% by other markers. As shown in Fig. 10, the data were still concentrated in the ranges 110–130 ka (~67%) and 80–90 ka (~15%), and the highest value of palaeo-RSL (33 ± 5 m MSL) was still related to a tectonically active area (area 16). If this area was removed from RSL reconstruction, the highest value of palaeo-RSL would decrease to 4.3 ± 0.75 m MSL for the period 110–130 ka and to 1.9 ± 0.75 m MSL for the period 80–90 ka.

To test the soundness of the employed selection criteria, we set progressively less stringent constraints for marine organisms (screening test II) which were most affected by the previous geochemical screening. Regarding the calcite content (criterion 1), about 90% of the screened data were rejected in screening test I because the calcite content was not determined by the original authors (Fig. 6A). Considering the large percentage, in screening test II we decided to reject only data with calcite content >3% and thus certainly altered. Nevertheless, only two samples of molluscs from a marine terrace in Spain (area 1) and a beach swash deposit in Israel (area 19) were added to the final keep-data group. Since the value of $\delta^{234}U_{initial}$ (criterion 3) was the most selective criterion (Fig. 6), we also decided to apply a wider range of 145 ± 15‰. Despite the large range adopted, only eight data were added to the data kept following the first more selective screening. These data referred to different RSL indicators (shallow or intertidal

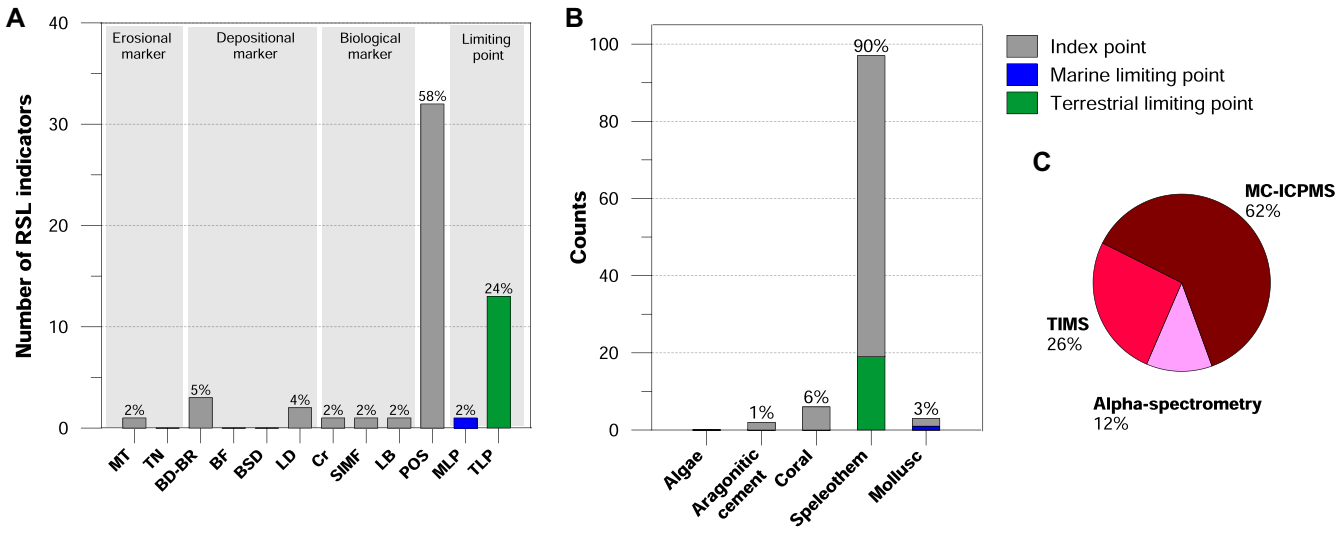

Figure 7. Statistics and distribution of the datapoints that passed geochemical screening: (A) number and percentage of RSL markers grouped per class (MT, marine terrace; TN, tidal notch; BD-BR, beach deposit or beachrock; BF, beach face; BSD, beach swash deposit; LD, littoral deposit; Cr, corals; SIMF, shallow or intertidal marine fauna; LB, upper limit of *Lithophaga* boreholes; POS, phreatic overgrowth on speleothems; MLP, marine limiting point; TLP, terrestrial limiting point); (B) type, number and percentage of material used to date the different RSL indicators; (C) percentage of analytical techniques adopted to date the material. In A and B index and limiting points are highlighted by different colours. [Color figure can be viewed at wileyonlinelibrary.com]

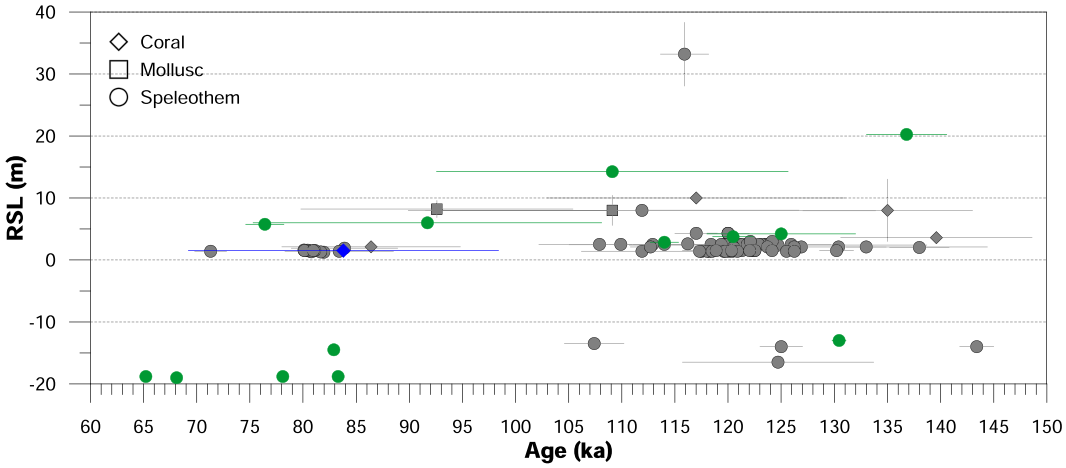

Figure 8. Altitudinal distribution and related age of the RSL indicators after the geochemical screening test I. In this graph, symbols indicate the type of dated material as reported in the legend while different colours indicate index datapoints (grey symbols), terrestrial limiting points (green symbols) and marine limiting points (blue symbols). The horizontal and vertical lines represent age and altitudinal uncertainties, respectively, reported as 2σ. [Color figure can be viewed at wileyonlinelibrary.com]

marine fauna, beach deposit or beachrock, littoral deposit and marine terrace) dated using corals (*Cladocora caespitosa*) and molluscs and located in Spain (areas 2, 3 and 4), Italy (area 10), Tunisia (area 15) and Greece (area 16). Since the less stringent screening test did not lead to significant changes, adding only 10 data, we can consider the criteria of screening I adequate and not too strict for marine organisms. Moreover, as the selected criteria of screening test I were already less stringent than those applied in other studies that also operated geochemical screenings on chronological data (Dutton and Lambeck, 2012; Medina-Elizalde, 2013; Hibbert *et al.*, 2016), we decided to set even more stringent constraints to the entire dataset (screening test III). Following the references cited above, we modified criteria 1, 3 and 4, selecting as reliable data with calcite content <2%, a range for $\delta^{234}U_{initial}$ of 145 ± 5‰ and $^{230}Th/^{232}Th$ activity ratio > 100, the last according to Richards and Dorale (2003). As expected, the application of stricter criteria in screening test III resulted in rejection of more samples compared with screening test I (21 additional data), for a total of ~73% of the entire dataset.

Discussion

A robust assessment of both the magnitude and temporal extent of the LIG sea-level highstand represents a key information to better constrain future sea-level scenarios in the current context of global warming (Kopp *et al.*, 2009). The newly assembled database, which includes 323 U/Th samples, provides a clearer picture of the reliability of LIG sea-level data in the Mediterranean area and shows how difficult it is to establish a reliable chronological framework.

Geochemical screening applied to chronological data indicates that caution should be used when the chronological attribution of MIS 5 outcrops is based only on U/Th dating on molluscs/corals for which a detailed screening has not been performed. For instance, about 97% of mollusc samples did not pass our screening to be considered reliable. This represents a major concern as the dated material is dominated by molluscs, which are more frequent than corals in the Quaternary marine invertebrate fossil record of Mediterranean shorelines. However, the less stringent screening test for marine organisms (screening test II), which would only add 10 markers to the final dataset,

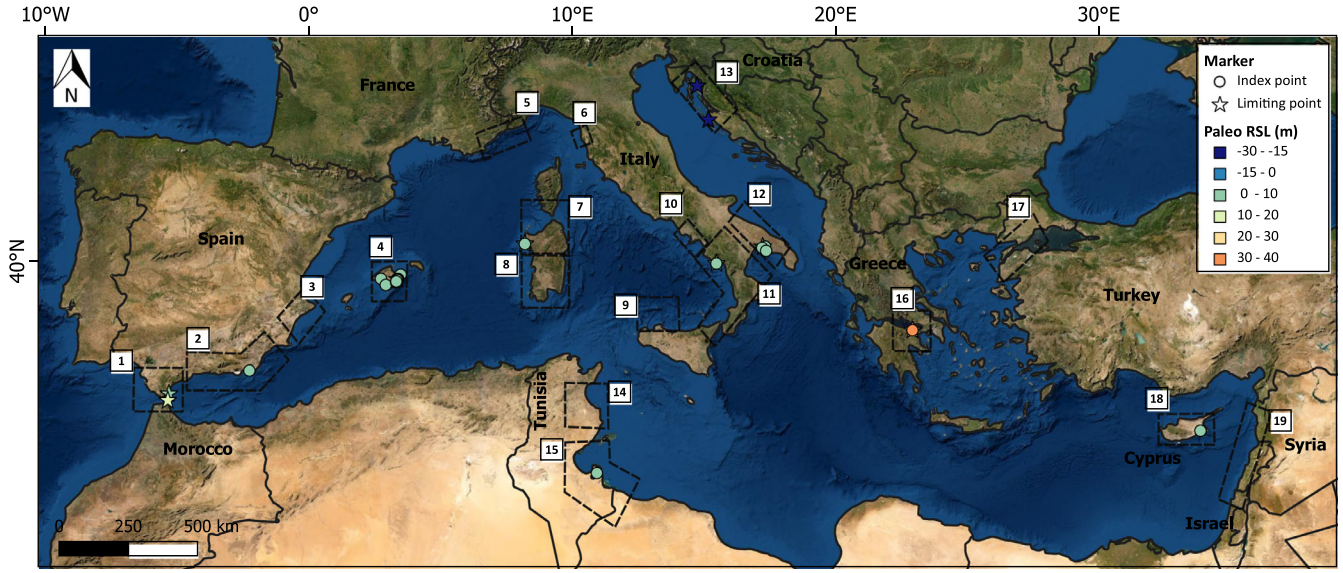

Figure 9. Localization and palaeo-RSL (m) of the markers that passed the geochemical screening. Index points are represented by dots while limiting points are represented by stars. The different colour of the datapoints indicates the range of their elevation in agreement with the colour-scale shown in the key. [Color figure can be viewed at wileyonlinelibrary.com]

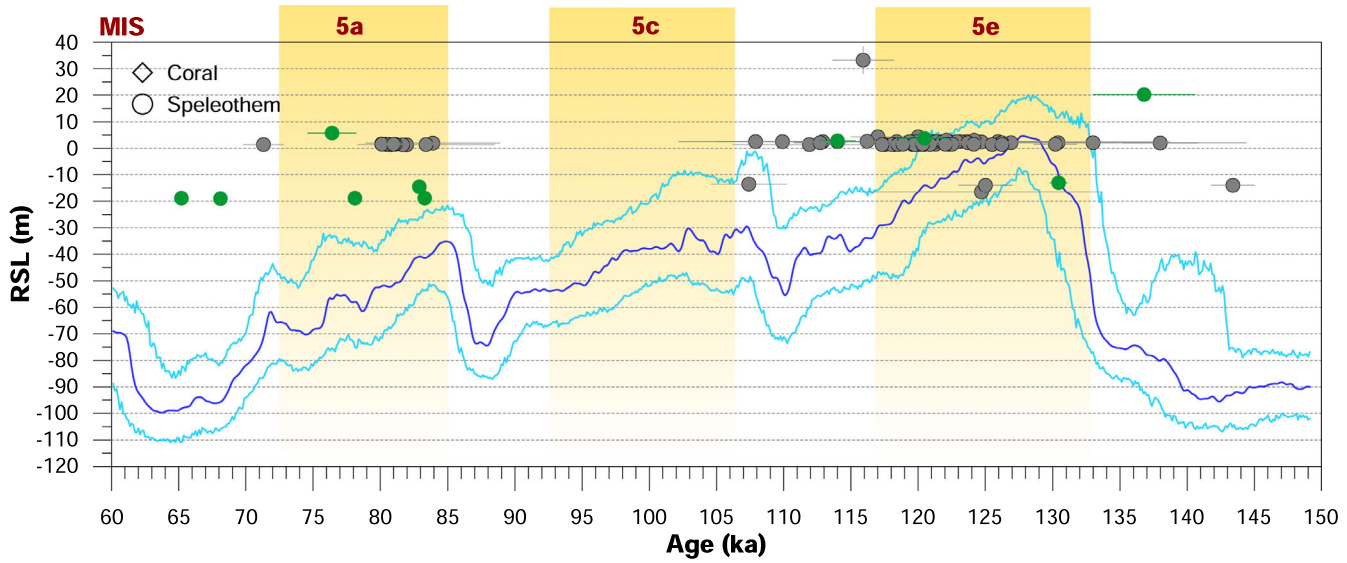

Figure 10. Altitudinal distribution and related age of the RSL indicators that passed the geochemical screening test I without alpha-spectrometry analysis, plotted together with the RSL record (dark blue curve) and the associated uncertainty (pale blue curves) of Grant *et al.* (2014). Temporal extent and boundaries of the MIS 5 substages are based on the LR04 benthic stack curve (Lisiecki and Raymo, 2005) according to Railsback *et al.* (2015). In this graph, symbols indicate the type of dated material as reported in the key while different colours indicate index datapoints (grey symbols) and terrestrial limiting points (green symbols). Horizontal and vertical lines represent age and altitudinal uncertainties, respectively, reported as 2σ. [Color figure can be viewed at wileyonlinelibrary.com]

pointed out that selected criteria are adequate and not too strict for these dated materials. By contrast, we should emphasize that speleothems are excluded from three out of four screening criteria and therefore the screening test is not so rigorous as for marine organisms. For speleothems, in addition to detrital Th contamination, detailed petrographic analysis (e.g. Bajo *et al.*, 2016) would also reveal evidence of potential diagenetic alteration and should be used to check their quality and integrity. Unfortunately, many studies did not perform this type of analysis and, even if performed, it would not be easy to set a criterion able to discriminate between petrographic characteristics and that can be applied in a dataset as a whole. However, if properly determined, it could represent a further test of quality.

Overall, the proposed selection of reliable/unreliable data would be useful for detecting areas where MIS 5 substage attributions are not supported by confident U/Th chronological data and for reviewing current implications based on data that did not pass our geochemical screening. As an example, in the area of Nice (France, area 5) there are only a few studies on LIG coastal shorelines based on U/Th dating (Stearns and Thurber, 1965; Dubar *et al.*, 2008; Gilli, 2018). Among them, Stearns and Thurber (1965) reported ages spanning from 75 to 110 ka for littoral deposits at very different elevations (between ca. 1.8 and 33.5 m a.s.l.). Dubar *et al.* (2008) also reported ages of ~130 ± 8 ka for beach deposits founded at ~16 and 10 m a.s.l. and proposed a reconstruction of the vertical tectonic movements since the LIG on the basis of the current elevation of these deposits. Unfortunately, the ages reported in the above-mentioned studies (mainly based on mollusc samples) were unreliable after our geochemical screening and, in addition, no other types of dating are available for this area. This has obvious consequences for tectonic interpretations reported in these studies and calls for an improvement of the chronology of the outcrops in the Nice area and a review of the current tectonic implications. More generally, none of the deposits attributed to MIS 5e along the Mediterranean coast of France (e.g. Ambert, 1999) and Corsica (e.g. Conchon, 1999) is currently supported by robust chronological data. Another example is provided by the Leghorn 'polycyclic Marine Terrace' in Tuscany (Italy, area 6) correlated with MIS 5 (Federici and Mazzanti, 1995). The local succession is characterized by two superimposed distinct marine/aeolian units, traditionally attributed to MIS 5e and MIS 5a/5c. In nearby sections, OSL (Mauz, 1999) and AAR (Hearty *et al.*, 1986b) dating partially support this view. However, Nisi *et al.* (2003) attributed this complex stratigraphic succession directly to MIS 5e in their reconstruction of the tectonic evolution of the Tyrrhenian coast. Recent U/Th measurements on *Cladocora caespitosa* carried out by Zanchetta *et al.* (2019) yielded ages between ~116 and 160 ka for some units of the Leghorn terrace, but according to our criteria these samples should be rejected. The chronology of this succession remains largely unsolved, even if the attribution of the lower unit to MIS 5e is supported by the presence of warm marine species. An additional example was recently reported for the Riparo Infreschi in Campania (Italy, area 11). Here, previous alpha-dating on vadose speleothems indicated that most of the local marine successions were related to MIS 5c (e.g. Esposito *et al.*, 2003). A new set of MC-ICPMS U/Th dates showed that there is a phase of marine deposition older than MIS 7 (possibly correlated with the highstand of MIS 9) and a younger phase related to MIS 5e (Bini *et al.*, 2020). These examples indicate that in the Mediterranean many stratigraphic reconstructions were based on unreliable chronological constraints, which misled any reconstructions of the tectonic or sea-level history. Figure 11 summarizes for each area selected in this study the percentage of unreliable/reliable data obtained after geochemical screening test I.

However, despite only 33% of the total geochronological data passing the screening test, most of which are speleothems, e.g. POS and subaerial speleothems (terrestrial limiting point) (Fig. 7), this does not mean that previous data are of no value. Indeed, different types of correction can be applied to avoid rejection of most dated samples. For instance, correction for $^{230}Th/^{232}Th$ detrital contamination is routinely done in many laboratories for speleothems (e.g. Schwarcz, 1989). Nevertheless, because the $^{230}Th/^{232}Th$ ratio varies considerably in the different Th source materials, it is not possible to correct measured ratios by a single, universally applicable initial $^{230}Th/^{232}Th$ ratio. Therefore, corrections may differ signifi-

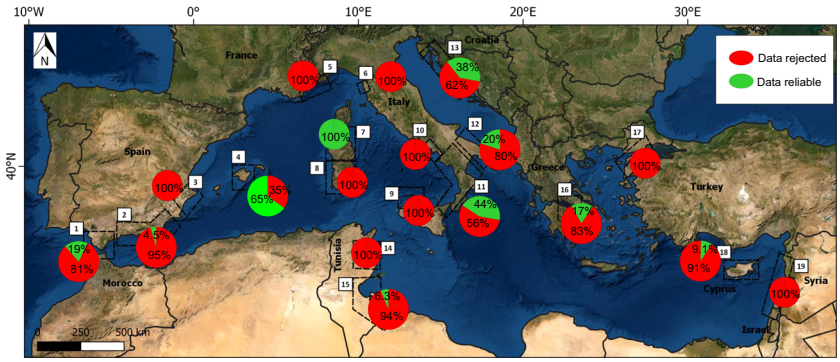

Figure 11. Summary of the percentage of unreliable/reliable data obtained after the geochemical screening test I for each area selected in this study. For information on samples, location and publications please refer to the database spreadsheet provided as a supplementary file. [Color figure can be viewed at wileyonlinelibrary.com]

cantly, according to the used approach (e.g. Hellstrom, 2006). Our rejections are thus independent of initial $^{230}Th/^{232}Th$ ratio corrections eventually applied in the original papers because we must be aware that proposed correction ages did not consider possible differences in the application of different corrections. Considering the $\delta^{234}U_{initial}$ value (criterion 3), this was the most selective criterion for molluscs and corals despite the wide range considered (145 ± 10‰) compared to other studies (Dutton and Lambeck, 2012; Medina-Elizalde, 2013; Hibbert *et al.*, 2016). This indicates that molluscs and corals rarely remained a closed system with respect to U-series decay nuclides during the post-emergence history, as it is well known for molluscs (e.g. Kaufman *et al.*, 1971; McLaren and Rowe, 1996). Therefore, some models for correct U-series ages with elevated $\delta^{234}U_{initial}$ values, and yielding an open-system age, were developed (Hille, 1979; Thompson *et al.*, 2003; Villemant and Feuillet, 2003; Scholz *et al.*, 2004). However, the scientific community is still divided regarding how such models may be appropriately applied to U/Th data (e.g. Stirling and Andersen, 2009). Moreover, all models should generally only be applied to coral data and there are some prerequisites for applying an open-system model on U/Th ages (e.g. Hibbert *et al.*, 2016). This correction was therefore not operated on the collected dataset as a whole. Nevertheless, we reported in the database the corrected age calculated by the original authors, which can be useful for different purposes. Figure 12 shows the final dataset presented in Fig. 10 along with data which did not pass our screening test I but were corrected and accepted by the different authors (67 samples referred to 35 RSL markers). We can note that the dataset is not significantly improved in terms of accuracy and precision of timing constraints.

Overall, our results (Figs. 8–10) indicate that the dataset of U/Th dating for the MIS 5 RSL of the Mediterranean basin is dramatically reduced to a third, or less, of the original one if rigorous geochemical screenings are applied. Moreover, we must keep in mind that due to the various diagenetic effects listed discussed and the high age uncertainties, corrected ages for molluscs could be used only for assignment to a given interglacial (Govin *et al.*, 2015). Corals could provide broad age constraints (e.g. Goy *et al.*, 2006), while achieving a millennial or sub-millennial resolution for the dating of corals of LIG age requires more efforts (Govin *et al.*, 2015). For example, some authors have shown that precise and reliable fossil coral ages could be obtained by dating the dense theca wall material of corals, which seems to be generally less affected by open-system behaviour than the bulk material commonly used for U/Th dating (e.g. Obert *et al.*, 2016), by dating multiple sub-samples of the same coral specimen (e.g. Scholz and Mangini, 2007), or by combining U/Th and Pa/U dating (e.g. Gallup *et al.*, 2002; Obert *et al.*, 2019). Furthermore, these techniques seem to be more rigorous in determining and detecting reliable ages for fossil corals than screening criteria, which in some cases have not been able to reveal all altered samples (e.g. Scholz and Mangini, 2007). This implies that the reliable dataset for the Mediterranean basin could be even smaller.

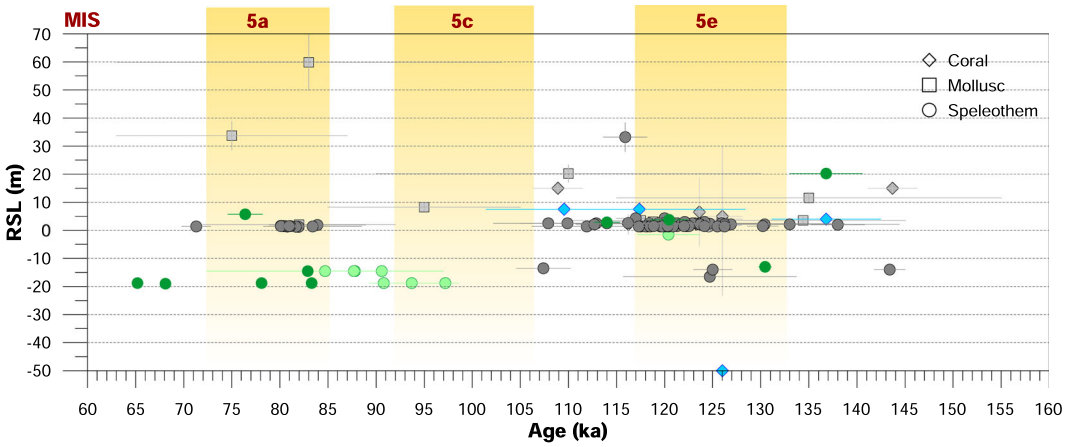

Figure 12. Altitudinal distribution and related age of the RSL indicators that passed geochemical screening along with data that did not pass the screening but were corrected and accepted by the original authors. Temporal extent and boundaries of the MIS 5 substages are based on the LR04 benthic stack curve (Lisiecki and Raymo, 2005) according to Railsback *et al.* (2015). In this graph, symbols indicate the type of dated material as reported in the key while different colours indicate index datapoints (grey for uncorrected reliable ages and light grey for corrected ages), terrestrial limiting points (green for uncorrected reliable ages and light green for corrected ages) and marine limiting points (light blue for corrected ages). Horizontal and vertical lines represent age and altitudinal uncertainties, respectively, reported as 2σ. [Color figure can be viewed at wileyonlinelibrary.com]

Most of the data that passed the screening test are located in the western Mediterranean where POS, which are the main RSL indicators (Fig. 7), occur quite frequently in the coastal karst caves of the area. In particular, most of these data (Fig. 9) come from Mallorca (area 4), which has been intensely investigated, both temporally and spatially, probably because of its assumed tectonic stability since the late Miocene and the richness of different types of well-preserved and datable RSL indicators (Lorscheid *et al.*, 2017). However, as briefly mentioned in the Introduction, the study of different RSL indicators from the island of Mallorca has led to contrasting results in terms of amplitude, timing and duration of the LIG highstand. For example, some authors have suggested the occurrence of two highstands, between 1.5 and 3.0 m MSL, that may have occurred from ~135 ka to 117–110-ka (Hillaire-Marcel *et al.*, 1996; Zazo *et al.*, 2003; Tuccimei *et al.*, 2007). Other authors have indicated a relatively stable RSL at 2.15 ± 0.75 m MSL, between ~126 and ~116 ka, with no rapid fluctuations and/or relatively long-stasis phases of sea-level at different elevations (Polyak *et al.*, 2018). In addition, while the dating of molluscs supported an attribution of RSL indicators to the MIS 5a/5c highstands ('Neotyrrhenian deposits'; e.g. Hillaire-Marcel *et al.*, 1996), coral dating made it possible to reinterpret the same deposits as different lithofacies of the same beach depositional unit belonging to MIS 5e ('Eutyrrehenian'; Muhs *et al.*, 2015). The selected chronological dataset obtained in this study (Fig. 10), which supposedly consists of reliable ages, highlights the presence of two highstands. The major one, which includes 70 datings (representing 65% of the final dataset) and spans the interval 130–108 ka with a weighted mean of 120 ± 14 ka, clearly matches MIS 5e. However, the lower boundary of this large cluster of dating overlaps the onset of the second MIS 5 peak of the RSL rising curve of the Red Sea, dated in this record at ~108 ka, which is probably correlated to the MIS 5c substage (Fig. 10). Therefore, considering the relatively large uncertainty associated with screened U/Th dating at ~108 ka, these could be either correlated to the end of MIS 5e or to the beginning of MIS 5c. However, our results show that no U/Th dating unambiguously falls within MIS 5c (107–95 ka) and that the dating encompassing the entire interval 130–108 ka shows no evident clustering in two distinct populations, possibly ascribable to MIS 5e and to the onset of MIS 5c (Fig. 10). In contrast, a second cluster of dating, including 18 datings (representing 17% of the final dataset) and spanning the interval 85–70 ka with a weighted mean of 80 ± 4 ka, is instead clearly correlated to the MIS 5a substage. However, Fig. 12 shows that a number of speleothems (despite being located in active tectonic context) corrected for detrital contamination indicate that RSL during MIS 5a/5c was significantly lower than RSL during MIS 5e, challenging the highstand identified in Mallorca during MIS 5a.

Finally, although several lines of regional geological, geomorphological and global proxy evidence suggest the presence of possible RSL oscillations during the LIG (e.g. Dabrio *et al.*, 2011; Sivan *et al.*, 2016; Rohling *et al.*, 2019), and considering the above-discussed data from Mallorca, the chronological dataset available for the Mediterranean gives no particular insight into either the chronology of the RSL oscillations within the LIG or its duration. This means that the current Mediterranean chronological dataset cannot be used for constraining the chronology of the LIG highstand on a regional scale, leaving open the questions and debate on the timing and dynamics of the LIG RSL oscillations. We note that in several sites other dating methods have been used to support chronological and stratigraphic attributions (e.g. Hearty *et al.*, 1986b; Mauz, 1999; Andreucci *et al.*, 2009). Of course, a multiproxy approach can ensure cross-control of age quality, even if this approach is not always able to improve the general accuracy and precision for defining the most cogent concerns for a detailed reconstruction and evolution of RSL during MIS5.

Concluding remarks

The application of different screening criteria on U/Th dating performed on Tyrrhenian LIG deposits of the Mediterranean coastline indicates that a significant number of past reconstructions were probably biased by chronological issues. This calls for a rethinking of some general paradigms, often uncritically accepted, such as the diffused presence of deposits related to MIS 5a/5c. Here we have shown that the majority (65%) of deposits that passed the geochemical screening test are likely to be related to MIS 5e, while only 17% of the chronological data for the MIS 5 highstand support a correlation to the MIS 5a substage. In contrast, our strict geochemical selection provides very poor chronological evidence of a relative highstand during the early part of the MIS 5c substage, which could be equally ascribed to MIS 5e because of the relatively large uncertainty of related U/Th dating. With the exception of the data from Mallorca, which do not support an unambiguous history, the data available do not allow a detailed definition of RSL evolution during the MIS 5e highstand in terms of duration and timing of the millennial-scale oscillations, representing an important challenge in the present scientific debate, also in consideration of future sea-level change.

From a methodological point of view, in light of future perspectives, the dataset proposed shows that the chronological framework available for the LIG RSL in the Mediterranean basin is far from satisfactory, despite the apparent large amount of data available. This dataset shows that if uncritically used, so many data can lead to a further increase in literature pollution, with a reiteration of unreliable data and interpretations. While great progress has been recently made in the standardization of definitions and measurements of RSL, the issue of dating remains, to a great extent, the greatest challenge. In this perspective, considering the conspicuous wealth of coastal MIS 5 records in the Mediterranean basin, which often provides rather well-preserved RSL markers, and the notable progress recently made in dating techniques, more efforts are needed to improve and obtain a reliable chronological framework for the LIG highstand. Re-examination of available samples that did not pass the geochemical screening with advanced techniques and decay constants might improve the quality of ancient data. Moreover, it may be good practice to report U-series data following the recommendations provided by Dutton *et al.* (2017) which specify the minimum set of required data to perform most calculations (and re-calculations) and facilitate later data comparisons. The acquisition of new U/Th measures following the advice reported, for example, in Obert *et al.* (2016) and Scholz and Mangini (2007) for corals (e.g. dating of multiple replicates and of the dense theca wall) and in Richards and Dorale (2003) for speleothems can lead to further improvements. In addition, the combined use of different dating methods, such as U/Th and Pa/U, applied on different sea-level markers (including terrestrial limiting points) would offer in the future fundamental insights into the LIG RSL history in the Mediterranean basin.

Acknowledgments. This research was financially supported by the Fondazione Cassa di Risparmio di Lucca ('Call 2016') within the project 'Clima ed eventi alluvionali estremi in Versilia: integrazione di nuove tecniche geoarcheologiche, geomorfologiche, geochimiche e simulazioni numeriche (Leader M.B.)'. The project was also funded by 'Fondi di Ateneo' University of Pisa (leaders G.Z. and M.B.) and is an integration of the targets of the PRIN 2017 'FUTURE Project' (MIUR grant no. 20177TKBXZ_003, Leader G.Z.).

Author Contributions—Conceptualization: F.P., M.B., A.R., G.Z.; Data curation: F.P., A.R., M.V.; Formal analysis: F.P.; Funding acquisition, M.B., G.Z.; Investigation: F.P., A.R.; Methodology: F.P., G.Z.; Project administration: M.B., G.Z.; Resources: M.B., G.Z.; Software: F.P., A.R.; Supervision: M.B., G.Z.; Validation: F.P., M.B., B.G., M.V., G.Z.; Visualization: F.P., B.G.; Writing – original draft: F.P., M.B., G.Z.; Writing – review and editing: B.G., A.R., M.V. All authors have read and agreed to the published version of the manuscript.

Conflicts of Interest—The authors declare no conflict of interest.

Supporting information

Additional supporting information can be found in the online version of this article.

Abbreviations. AAR, amino acid racemization; LIG, Last Interglacial; MIS, Marine Isotopic Stage; MLP, marine limiting point; OSL, optical stimulated luminescence; POS, phreatic overgrowths on speleothems; RSL, relative sea level; WALIS, World Atlas of Last Interglacial Shorelines.

References

Abad M, Rodríguez-Vidal J, Aboumaria K *et al*. 2013. Evidence of MIS 5 sea-level highstands in Gebel Mousa coast (Strait of Gibraltar, North of Africa). *Geomorphology* **182**: 133–146.

Alİyev SA, Sari A. 2003. Biogenic accumulations of uranium in recent seas. *Acta Geologica Sinica - English Edition* **77**: 372–381.

Ambert P. 1999. Les formations littorales pléistocènes du Languedoc [Pleistocene shorelines of Languedoc]. *Quaternaire* **10**: 83–93.

Amorosi A, Antonioli F, Bertini A *et al*. 2014. The Middle–Upper Pleistocene Fronte Section (Taranto, Italy): an exceptionally preserved marine record of the Last Interglacial. *Global and Planetary Change* **119**: 23–38.

Andersen MB, Stirling CH, Zimmermann B *et al*. 2010. Precise determination of the open ocean 234U/238U composition. *Geochemistry, Geophysics, Geosystems* **11**.

Andreucci S, Pascucci V, Murray AS *et al*. 2009. Late Pleistocene coastal evolution of San Giovanni di Sinis, west Sardinia (Western Mediterranean). *Sedimentary Geology* **216**: 104–116.

Andrews JE, Portman C, Rowe PJ *et al*. 2007. Sub-orbital sea-level change in early MIS 5e: new evidence from the Gulf of Corinth, Greece. *Earth and Planetary Science Letters* **259**: 457–468.

Antonioli F, Ferranti L, Stocchi P *et al*. 2018. Morphometry and elevation of the last interglacial tidal notches in tectonically stable coasts of the Mediterranean Sea. *Earth-Science Reviews* **185**: 600–623.

Antonioli F, Lo Presti V, Rovere A *et al*. 2015. Tidal notches in Mediterranean Sea: a comprehensive analysis. *Quaternary Science Reviews* **119**: 66–84.

Asioli A, Capotondi L, Sironi MBC. 2005. The Tyrrhenian stage in the Mediterranean: definition, usage and recognition in the deep-sea record. A proposal. *Rendiconti Lincei* **16**: 297–310.

Bajo P, Hellstrom J, Frisia S *et al*. 2016. "Cryptic" diagenesis and its implications for speleothem geochronologies. *Quaternary Science Reviews* **148**: 17–28.

Barra D, Cinque A, Gewelt M *et al*. 1991. L'ospite caldo Silvestra seminis (Bonaduce, Masoli e Pugliese, 1976) (Crustacea, Ostracoda): un possibile marker dell'ultimo interglaciale dell'area mediterranea. *Quat* **4**: 327–332.

Belluomini G, Caldara M, Casini C *et al*. 2002. The age of Late Pleistocene shorelines and tectonic activity of Taranto area, southern Italy. *Quaternary Science Reviews* **21**: 525–547.

Billi A, Faccenna C, Bellier O *et al*. 2011. Recent tectonic reorganization of the Nubia-Eurasia convergent boundary heading for the closure of the western Mediterranean. *Bulletin de la Société Géologique de France* **182**: 279–303.

Bini M, Zanchetta G, Drysdale RN *et al*. 2020. An end to the Last Interglacial highstand before 120 ka: relative sea-level evidence from Infreschi Cave (Southern Italy). *Quaternary Science Reviews* **250**. [PubMed: 106658]

Bonifay E, Mars P. 1959. Le Tyrrhenien dans le cadre de la chronologie quaternaire mediterraneenne. *Bull. la Société Géologique Fr.* **S7-I**: 62–75.

Brancaccio L, Capaldi G, Cinque A *et al*. 1978. 230Th −234U dating of corals from a Tyrrhenian beach in Sorrentine peninsula (Southern Italy). *Quaternaria* **20**: 175–183.

Broecker WS. 1963. A preliminary evaluation of uranium series inequilibrium as a tool for absolute age measurement on marine carbonates. *Journal of Geophysical Research* **68**: 2817–2834.

Burke KD, Williams JW, Chandler MA *et al*. 2018. Pliocene and Eocene provide best analogs for near-future climates. *Proceedings of the National Academy of Sciences of the United States of America* **115**: 13288–13293. [PubMed: 30530685]

Carboni S, Lecca L, Hillaire-Marcel C *et al*. 2014. MIS 5e at San Giovanni di Sinis (Sardinia, Italy): stratigraphy, U/Th dating and 'eustatic' inferences. *Quaternary International* **328–329**: 21–30.

Chen S, Littley EFM, Rae JWB *et al*. 2021. Uranium distribution and incorporation mechanism in deep-sea corals: implications for seawater [CO_3^{2-}. *Frontiers in Earth Science* **9**: 159.

Cheng H, Lawrence Edwards R, Shen CC *et al*. 2013. Improvements in 230Th dating, 230Th and 234U half-life values, and U-Th isotopic measurements by multi-collector inductively coupled plasma mass spectrometry. *Earth and Planetary Science Letters* **371–372**: 82–91.

Chutcharavan PM, Dutton A, Ellwood MJ. 2018. Seawater $^{234}U/^{238}U$ recorded by modern and fossil corals. *Geochimica et Cosmochimica Acta* **224**: 1–17.

Clark PU, Shakun JD, Marcott SA *et al*. 2016. Consequences of twenty-first-century policy for multi-millennial climate and sea-level change. *Nature Climate Change* **6**: 360–369.

Coltorti M, Pieruccini P, Montagna P *et al*. 2015. Stratigraphy, facies analysis and chronology of Quaternary deposits at Capo S. Marco (Sinis Peninsula, west Sardinia, Italy). *Quaternary International* **357**: 158–175.

Conchon O. 1999. Le littoral de Corse (France) au Quaternaire [Corsica coast (France, Western Mediterranea) during the Quaternary]. *Quaternaire* **10**: 95–105.

D'Orefice M, Graciotti R, Lo Mastro S *et al*. 2012. U/Th dating of a Cladocora caespitosa from Capo San Marco marine Quaternary deposits (Sardinia, Italy). Alp. *Mediterranean Quarterly* **25**: 35–40.

Dabrio CJ, Zazo C, Cabero A *et al*. 2011. Millennial/submillennial-scale sea-level fluctuations in western Mediterranean during the second highstand of MIS 5e. *Quaternary Science Reviews* **30**: 335–346.

Dai Pra G, Miyauchi T, Anselmi B *et al*. 1993. Età dei depositi a Strombus bubonious di Vibo Valentia Marina (Italia Meridionale). *Quat* **6**: 139–144.

Dai Pra G, Stearns CE. 1977. Sul Tirreniano di Taranto. Datazioni su coralli con il metodo del TH230/U234. *Geol Rom* **16**: 231–242.

De Vita S, Laurenzi MA, Orsi G *et al*. 1998. Application of $^{40}Ar/^{39}Ar$ and ^{230}Th dating methods to the chronostratigraphy of quaternary basaltic volcanic areas: the Ustica island case history. *Quaternary International* **47–48**: 117–127.

Delanghe D, Bard E, Hamelin B. 2002. New TIMS constraints on the uranium-238 and uranium-234 in seawaters from the main ocean basins and the Mediterranean Sea. *Marine Chemistry* **80**: 79–93.

Dia AN, Cohen AS, O'Nions RK *et al*. 1997. Rates of uplift investigated through 230th dating in the Gulf of Corinth (Greece). *Chemical Geology* **138**: 171–184.

Dodonov AE, Trifonov VG, Ivanova TP *et al*. 2008. Late Quaternary marine terraces in the Mediterranean coastal area of Syria: geochronology and neotectonics. *Quaternary International* **190**: 158–170.

Dorale JA, Onac BP, Fornós JJ *et al*. 2010. Sea-level highstand 81,000 years ago in Mallorca. *Science* **327**: 860–863. This [PubMed: 20150501]

Dubar M, Innocent C, Sivan O. 2008. Radiometric dating (U/Th) of the lower marine terrace (MIS 5.5) west of Nice (French Riviera): morphological and neotectonic quantitative implications. *Comptes Rendus Geoscience* **340**: 723–731.

Dumitru OA, Polyak VJ, Asmerom Y *et al*. 2020. Last Interglacial (sensu lato, ~130 to 75 ka) sea level history from cave deposits: a global standardized database. *Earth System Science Data Discussions* **4313861**: 1–25.

Durand N, Deschamps P, Bard E *et al*. 2013. Comparison of 14C and U-T Ages in corals from IODP #310 cores offshore Tahiti. *Radiocarbon* **55**: 1947–1974.

Dutton A. 2015. Uranium–thorium dating. In *Handbook of Sea-Level Research*, Shennan I, Long AJ, Horton BP (eds). Wiley: London; 386.

Dutton A, Carlson AE, Long AJ *et al*. 2015. Sea-level rise due to polar ice-sheet mass loss during past warm periods. *Science* **349**: aaa4019. https://doi.org/10.1126/science.aaa4019. [PubMed: 26160951]

Dutton A, Lambeck K. 2012. Ice volume and sea level during the last interglacial. *Science* **337**: 216–219. [PubMed: 22798610]

Dutton A, Rubin K, McLean N *et al*. 2017. Data reporting standards for publication of U-series data for geochronology and timescale assessment in the earth sciences. *Quaternary Geochronology* **39**: 142–149.

El Abdellaoui JEE, Petit F, Ghaleb B *et al*. 2016. Sea-level fluctuation during MIS 5e and geomorphological context on the southern coast of the Strait of Gibraltar (Morocco). *Géomorphologie: Relief, Processus, Environnement* **22**: 287–301.

El Kadiri K, de Galdeano CS, Pedrera A *et al*. 2010. Eustatic and tectonic controls on Quaternary Ras Leona marine terraces (Strait of Gibraltar, northern Morocco). *Quaternary Research* **74**: 277–288.

Esat TM, Yokoyama Y. 2006. Variability in the uranium isotopic composition of the oceans over glacial–interglacial timescales. *Geochimica et Cosmochimica Acta* **70**: 4140–4150.

Esposito C, Filocamo F, Marciano R *et al* 2003. Late Quaternary shorelines in southern Cilento (Mt. Bulgheria): morphostratigraphy and chronology. *Quat* **16**: 3–14.

Faccenna C, Becker TW, Auer L *et al*. 2014. Mantle dynamics in the Mediterranean. *Reviews of Geophysics* **52**: 283–332.

Federici PR, Mazzanti R. 1995. Note sulle pianure costiere della Toscana. Mem. della. *Social Geography Ital*. **53**: 165–270.

Ferranti L, Antonioli F, Mauz B *et al*. 2006. Markers of the last interglacial sea-level high stand along the coast of Italy: tectonic implications. *Quaternary International* **145–146**: 30–54.

Fortunato H. 2016. Mollusks: tools in environmental and climate research. *American Malacological Bulletin* **33**: 310–324.

Galli P. 2020. Recurrence times of central-southern Apennine faults (Italy): hints from palaeoseismology. *Terra Nova* **32**: 399–407.

Gallup CD, Cheng H, Taylor FW *et al*. 2002. Direct determination of the timing of sea level change during termination II. *Science* **295**: 310–313. [PubMed: 11786639]

Gallup CD, Edwards RL, Johnson RG. 1994. The timing of high sea levels over the past 200,000 years. *Science* **263**: 796–800. [PubMed: 17770835]

Gilli E. 2018. Karstodyssée 2016, Analyse des marqueurs eustatiques, tectoniques et tsunamiques dans les karsts littoraux méditerranéens. Nice. https://doi.org/10.13140/RG.2.2.33426.15048

Govin A, Capron E, Tzedakis PC *et al*. 2015. Sequence of events from the onset to the demise of the Last Interglacial: evaluating strengths and limitations of chronologies used in climatic archives. *Quaternary Science Reviews* **129**: 1–36.

Goy JL, Hillaire-Marcel C, Zazo C *et al*. 2006. Further evidence for a relatively high sea level during the penultimate interglacial: open-system U-series ages from la Marina (Alicante, East Spain). *Geodinamica Acta* **19**: 409–426.

Grant KM, Rohling EJ, Ramsey CB *et al*. 2014. Sea-level variability over five glacial cycles. *Nature Communications* **5**: 5076. [PubMed: 25254503]

Hearty PJ. 1986. An inventory of last Interglacial (sensu lato) age deposits from the Mediterranean basin: a study of isoleucine epimerization and U- series dating. *Zeitschrift fur Geomorphol. Suppl.-Bd* 51–69.

Hearty PJ, Bonfiglio L, Violanti D *et al*. 1986a. Age of late Quaternary marine deposits of southern Italy determined by aminostratigraphy, faunal correlation, and uranium-series dating. *Rivista, Italiana di Paleontologiia e Stratigrafia* **92**: 149–164.

Hearty PJ, Hollin JT, Neumann AC *et al*. 2007. Global sea-level fluctuations during the Last Interglaciation (MIS 5e). *Quaternary Science Reviews* **26**: 2090–2112.

Hearty PJ, Miller GH, Stearns CE *et al*. 1986b. Aminostratigraphy of Quaternary shorelines in the Mediterranean basin. *Geological Society of America Bulletin* **97**: 850–858.

Hellstrom J. 2003. Rapid and accurate U/Th dating using parallel ion-counting multi-collector ICP-MS. *Journal of Analytical Atomic Spectrometry* **18**: 1346–1351.

Hellstrom J. 2006. U–Th dating of speleothems with high initial ^{230}Th using stratigraphical constraint. *Quaternary Geochronology* **1**: 289–295.

Henderson GM. 2002. Seawater (^{234}U/^{238}U) during the last 800 thousand years. *Earth and Planetary Science Letters* **199**: 97–110.

Hibbert FD, Rohling EJ, Dutton A *et al*. 2016. Coral indicators of past sea-level change: A global repository of U-series dated benchmarks. *Quaternary Science Reviews* **145**: 1–56.

Hillaire-Marcel C, Carro O, Causse C *et al*. 1986. Th/U dating of *Strombus bubonius*-bearing marine terraces in southeastern Spain. *Geology* **14**: 613–616.

Hillaire-Marcel C, Gariépy C, Ghaleb B *et al*. 1996. U-series measurements in Tyrrhenian deposits from Mallorca – Further evidence for two last-interglacial high sea levels in the Balearic Islands. *Quaternary Science Reviews* **15**: 53–62.

Hille P. 1979. An open system model for uranium series dating. *Earth and Planetary Science Letters* **42**: 138–142.

IAEA. 1989. Technical Reports, Series No: **295**.

Iannace A, Romano P, Santangelo N *et al*. 2001. The OIS 5c along Licosa cape promontory (campania region, southern Italy): morphostratigraphy and U/Th dating. *Zeitschrift für Geomorphologie* **45**: 307–319.

Issel A. 1914. Lembi fossiliferi quaternarie recenti nella Sardegna meridionale. *Accad Naz dei Lincei* **5**: 759–770.

Ivanovich M, Vita-Finzi C, Hennig GJ. 1983. Uranium-series dating of molluscs from uplifted Holocene beaches in the Persian Gulf. *Nature* **302**: 408–410.

Jedoui Y, Reyss JL, Kallel N *et al*. 2003. U-series evidence for two high Last Interglacial sea levels in southeastern Tunisia. *Quaternary Science Reviews* **22**: 343–351.

Kaufman A, Broecker WS, Ku T-L *et al*. 1971. The status of U-series methods of mollusk dating. *Geochimica et Cosmochimica Acta* **35**: 1155–1183.

Kopp RE, Simons FJ, Mitrovica JX *et al*. 2009. Probabilistic assessment of sea level during the last interglacial stage. *Nature* **462**: 863–867. [PubMed: 20016591]

Lambeck K, Bard E. 2000. Sea-level change along the French Mediterranean coast for the past 30 000 years. *Earth and Planetary Science Letters* **175**: 203–222.

Leeder MR, McNeill LC, Ll Collier RE *et al*. 2003. Corinth rift margin uplift: new evidence from Late Quaternary marine shorelines. *Geophysical Research Letters* **30**: 4–7.

Leeder MR, Portman C, Andrews JE *et al*. 2005. Normal faulting and crustal deformation, Alkyonides Gulf and Perachora peninsula, eastern Gulf of Corinth rift, Greece. *Journal of the Geological Society* **162**: 549–561.

Li W-X, Lundberg J, Dickin AP *et al*. 1989. High-precision mass-spectrometric uranium-series dating of cave deposits and implications for palaeoclimate studies. *Nature* **339**: 534–536.

Lisiecki LE, Raymo ME. 2005. A Pliocene–Pleistocene stack of 57 globally distributed benthic δ 18O records. *Paleoceanography* **20**.

Lorscheid T, Stocchi P, Casella E *et al*. 2017. Paleo sea-level changes and relative sea-level indicators: precise measurements, indicative meaning and glacial isostatic adjustment perspectives from Mallorca (western Mediterranean). *Palaeogeography, Palaeoclimatology, Palaeoecology* **473**: 94–107.

Marra F, Bahain J-J, Jicha BR *et al*. 2019. Reconstruction of the MIS 5.5, 5.3 and 5.1 coastal terraces in Latium (central Italy): A re-evaluation of the sea-level history in the Mediterranean Sea during the last interglacial. *Quaternary International* **525**: 54–77.

Mauz B. 1999. Late Pleistocene records of littoral processes at the Tyrrhenian Coast (Central Italy): depositional environments and luminescence chronology. *Quaternary Science Reviews* **18**: 1173–1184.

McLaren SJ, Rowe PJ. 1996. The reliability of uranium-series mollusc dates from the western Mediterranean basin. *Quaternary Science Reviews* **15**: 709–717.

Medina-Elizalde M. 2013. A global compilation of coral sea-level benchmarks: implications and new challenges. *Earth and Planetary Science Letters* **362**: 310–318.

Montagna P, McCulloch M, Mazzoli C *et al*. 2007. The non-tropical coral Cladocora caespitosa as the new climate archive for the Mediterranean: high-resolution (~weekly) trace element systematics. *Quaternary Science Reviews* **26**: 441–462.

Muhs DR. 2002. Evidence for the timing and duration of the last interglacial period from high-precision uranium-series ages of corals on tectonically stable coastlines. *Quaternary Research* **58**: 36–40.

Muhs DR, Simmons KR, Meco J *et al*. 2015. Uranium-series ages of fossil corals from Mallorca, Spain: the 'Neotyrrhenian' high stand of the Mediterranean Sea revisited. *Palaeogeography, Palaeoclimatology, Palaeoecology* **438**: 408–424.

Negri A, Amorosi A, Antonioli F *et al*. 2015. A potential global boundary stratotype section and point (GSSP) for the Tarentian Stage, Upper Pleistocene, from the Taranto area (Italy): results and future perspectives. *Quaternary International* **383**: 145–157.

Nisi MF, Antonioli F, Pra GD *et al*. 2003. Coastal deformation between the Versilia and the Garigliano plains (Italy) since the last interglacial stage. *Journal of Quaternary Science* **18**: 709–721.

Nocquet JM. 2012. Present-day kinematics of the Mediterranean: A comprehensive overview of GPS results. *Tectonophysics* **579**: 220–242.

O'Leary MJ, Hearty PJ, Thompson WG *et al*. 2013. Ice sheet collapse following a prolonged period of stable sea level during the last interglacial. *Nature Geoscience* **6**: 796–800.

Obert JC, Scholz D, Felis T *et al*. 2016. ^{230}Th/U dating of Last Interglacial brain corals from Bonaire (southern Caribbean) using bulk and theca wall material. *Geochimica et Cosmochimica Acta* **178**: 20–40.

Obert JC, Scholz D, Felis T *et al*. 2019. Improved constraints on open-system processes in fossil reef corals by combined Th/U, Pa/U and Ra/Th dating: A case study from Aqaba, Jordan. *Geochimica et Cosmochimica Acta* **245**: 459–478.

Past Interglacials Working Group of PAGES. 2016. Interglacials of the last 800,000 years. *Reviews of Geophysics* **54**: 162–219.

Polyak VJ, Onac BP, Fornós JJ *et al*. 2018. A highly resolved record of relative sea level in the western Mediterranean Sea during the last interglacial period. *Nature Geoscience* **11**: 860–864.

Poole AJ, Shimmield GB, Robertson AHF. 1990. Late Quaternary uplift of the Troodos ophiolite, Cyprus: uranium- series dating of Pleistocene coral. *Geology* **18**: 894–897.

Raddatz J, Rüggeberg A, Flögel S *et al*. 2014. The influence of seawater pH on U/Ca ratios in the scleractinian cold-water coral *Lophelia pertusa*. *Biogeosciences* **11**: 1863–1871.

Railsback LB, Gibbard PL, Head MJ *et al*. 2015. An optimized scheme of lettered marine isotope substages for the last 1.0 million years, and the climatostratigraphic nature of isotope stages and substages. *Quaternary Science Reviews* **111**: 94–106.

Ratti A. 2019 *Le Variazioni del Livello del Mare Relativo durante il MIS 5e nel Mar Mediterraneo, Nuovi Dati da Grotta degli Infreschi*. Thesis, University of Pisa (in Italian).

Richards DA, Dorale JA. 2003. Uranium-series chronology and environmental applications of speleothems. *Reviews in Mineralogy and Geochemistry* **52**: 407–460.

Roberts GP, Houghton SL, Underwood C *et al*. 2009. Localization of quaternary slip rates in an active rift in 105 years: an example from central Greece constrained by ^{234}U- ^{230}Th coral dates from uplifted paleoshorelines. *Journal of Geophysical Research* **114**: 1–26.

Rohling EJ, Hibbert FD, Grant KM *et al*. 2019. Asynchronous Antarctic and Greenland ice-volume contributions to the last interglacial sea-level highstand. *Nature Communications* **10**: 5040. [PubMed: 31695032]

Romano P, Santo A, Voltaggio M. 1994. L'evoluzione geomorfologica della pianura del fiume Volturno (Campania) durante il tardo Quaternario (Pleistocene Medio-Superiore – Olocene). *Quat* **7**: 41–55.

Rovere A, Raymo ME, Vacchi M *et al*. 2016. The analysis of Last Interglacial (MIS 5e) relative sea-level indicators: reconstructing sea-level in a warmer world. *Earth-Science Reviews* **159**: 404–427.

Rovere A, Ryan D & Murray-Wallace C et al. 2020. Descriptions of Database Fields for the World Atlas of Last Interglacial Shorelines (WALIS). https://doi.org/10.5281/zenodo.3961544

Sarti G, Zanchetta G, Ciulli L *et al*. 2005. Late Quaternary oligotypical non-marine mollusc fauna from southern Tuscany: climatic and stratigraphic implications. *Geologica Acta* **4**: 159–167.

Scholz D, Mangini A. 2007. How precise are U-series coral ages? *Geochimica et Cosmochimica Acta* **71**: 1935–1948.

Scholz D, Mangini A, Felis T. 2004. U-series dating of diagenetically altered fossil reef corals. *Earth and Planetary Science Letters* **218**: 163–178.

Schwarcz HP. 1989. Uranium series dating of Quaternary deposits. *Quaternary International* **1**: 7–17.

Serpelloni E, Faccenna C, Spada G *et al*. 2013. Vertical GPS ground motion rates in the Euro-Mediterranean region: new evidence of velocity gradients at different spatial scales along the Nubia-Eurasia plate boundary. *Journal of Geophysical Research: Solid Earth* **118**: 6003–6024.

Shackleton NJ. 1969. The last interglacial in the marine and terrestrial records. *Proceedings of the Royal Society of London Series B* **174**: 135–154.

Shennan I, Long A, Horton BP. 2015. *Handbook of Sea-Level Research*. John Wiley & Sons, Ltd: Chichester.

Sivan D, Sisma-Ventura G, Greenbaum N *et al*. 2016. Eastern Mediterranean sea levels through the last interglacial from a coastal-marine sequence in northern Israel. *Quaternary Science Reviews* **145**: 204–225.

Stearns CE, Thurber DL. 1965. Th230/U234 dates of Late Pleistocene marine fossils from the Mediterranean and Moroccan littorals. *Progress in Oceanography* **4**: 293–305.

Steffen W, Rockström J, Richardson K *et al*. 2018. Trajectories of the Earth system in the Anthropocene. *Proceedings of the National Academy of Sciences of the United States of America* **115**: 8252–8259. [PubMed: 30082409]

Stirling CH, Andersen MB. 2009. Uranium-series dating of fossil coral reefs: extending the sea-level record beyond the last glacial cycle. *Earth and Planetary Science Letters* **284**: 269–283.

Stirling CH, Esat TM, Lambeck K *et al*. 1998. Timing and duration of the Last Interglacial: evidence for a restricted interval of widespread coral reef growth. *Earth and Planetary Science Letters* **160**: 745–762.

Stirling CH, Esat TM, Lambeck K *et al*. 2001. Orbital forcing of the marine isotope Stage 9 interglacial. *Science* **291**: 290–293. [PubMed: 11209076]

Stocchi P, Vacchi M, Lorscheid T *et al*. 2018. MIS 5e relative sea-level changes in the Mediterranean Sea: contribution of isostatic disequilibrium. *Quaternary Science Reviews* **185**: 122–134.

Surić M, Juračić M. 2010. Late Pleistocene – Holocene environmental changes – records from submerged speleothems along the Eastern Adriatic coast (Croatia). *Geologia Croatica* **63**: 155–169.

Taviani M. 2014. Unpersisting Persististrombus: a Mediterranean story. *Vieraea Folia Sci. Biol Canar* 9–18.

Thompson WG, Spiegelman MW, Goldstein SL *et al*. 2003. An open-system model for U-series age determinations of fossil corals. *Earth and Planetary Science Letters* **210**: 365–381.

Tuccimei P, Fornós JJ, Ginés Á *et al*. 2007. Sea level change at Capo Caccia (NW Sardinia) and Mallorca (Balearic Islands) during oxygen isotope substage 5e, based on Th/U datings of phreatic overgrowths on speleothems. Geomorfol. litoral i Quat. *Homenatge à Joan Cuerda Barceló* 121–135.

Tzedakis PC, Drysdale RN, Margari V *et al*. 2018. Enhanced climate instability in the North Atlantic and southern Europe during the Last Interglacial. *Nature Communications* **9**: 4235. [PubMed: 30315157]

Tzedakis PC, Raynaud D, McManus JF *et al*. 2009. Interglacial diversity. *Nature Geoscience* **2**: 751–755.

Vacchi M, Marriner N, Morhange C *et al*. 2016. Multiproxy assessment of Holocene relative sea-level changes in the western Mediterranean: sea-level variability and improvements in the definition of the isostatic signal. *Earth-Science Reviews* **155**: 172–197.

Vesica PL, Tuccimei P, Turi B *et al*. 2000. Late Pleistocene Paleoclimates and sea-level change in the Mediterranean as inferred from stable isotope and U-series studies of overgrowths on speleothems, Mallorca, Spain. *Quaternary Science Reviews* **19**: 865–879.

Villemant B, Feuillet N. 2003. Dating open systems by the 238U–234U-230Th method: application to Quaternary reef terraces. *Earth and Planetary Science Letters* **210**: 105–118.

Vita-Finzi C. 1993. Evaluating Late Quaternary uplift in Greece and Cyprus. *Geological Society, London, Special Publications* **76**: 417–424.

Yaltirak C, Sakinç M, Aksu AE *et al*. 2002. Late Pleistocene uplift history along the southwestern Marmara Sea determined from raised coastal deposits and global sea-level variations. *Marine Geology* **190**: 283–305.

Zanchetta G, Bini M, Montagna P *et al*. 2019. Stable isotope composition of fossil ahermatypic coral *Cladocora caespitosa* (L.) from Pleistocene raised marine terraces of the livorno area (Central Italy). Alp. *Mediterranean Quarterly* **32**: 73–86.

Zazo C, Goy JL, Dabrio CJ *et al*. 2003. Pleistocene raised marine terraces of the Spanish Mediterranean and Atlantic Coasts: records of coastal uplift, sea-level highstands and climate changes. *Marine Geology* **194**: 103–133.

Zazo C, Silva PG, Goy JL *et al*. 1999. Coastal uplift in continental collision plate boundaries: data from the Last Interglacial marine terraces of the Gibraltar Strait area (south Spain). *Tectonophysics* **301**: 95–109.

